

Geodinamica Acta

ISSN: 0985-3111 (Print) 1778-3593 (Online) Journal homepage: https://www.tandfonline.com/loi/tgda20

Geochemical characteristics of ophiolitic rocks from the southern margin of the Sivas basin and their implications for the Inner Tauride Ocean, Central-Eastern Turkey

Kaan Şevki Kavak, Osman Parlak & Haluk Temiz

To cite this article: Kaan Şevki Kavak, Osman Parlak & Haluk Temiz (2017) Geochemical characteristics of ophiolitic rocks from the southern margin of the Sivas basin and their implications for the Inner Tauride Ocean, Central-Eastern Turkey, Geodinamica Acta, 29:1, 160-180, DOI: 10.1080/09853111.2017.1359773

To link to this article: https://doi.org/10.1080/09853111.2017.1359773

© 2017 The Author(s). Published by Informa UK Limited, trading as Taylor & Francis Group

View supplementary material

Published online: 13 Sep 2017.

Submit your article to this journal

Article views: 876

View related articles

View Crossmark data

Citing articles: 3 View citing articles

Full Terms & Conditions of access and use can be found at
https://www.tandfonline.com/action/journalInformation?journalCode=tgda20

GEODINAMICA ACTA, 2017
VOL. 29, NO. 1, 160–180
https://doi.org/10.1080/09853111.2017.1359773

Taylor & Francis
Taylor & Francis Group

OPEN ACCESS Check for updates

Geochemical characteristics of ophiolitic rocks from the southern margin of the Sivas basin and their implications for the Inner Tauride Ocean, Central-Eastern Turkey

Kaan Şevki Kavak[a], Osman Parlak[b] and Haluk Temiz[a]

[a]Jeoloji Mühendisliği Bölümü, Cumhuriyet Üniversitesi, Sivas, Turkey; [b]Jeoloji Mühendisliği Bölümü, Çukurova Üniversitesi, Adana, Turkey

ABSTRACT

Number of dismembered ophiolite bodies crop out between Sivas and Malatya on the top of the Eastern Tauride platform in the central-eastern Turkey. One of which at the southern margin of the Sivas basin in the Tecer Mountain area comprises melange and the lower part of an oceanic lithospheric section on top of the Tauride platform. The mantle tectonites are characterized by variably serpentinized harzburgites and dunites, and are intruded by numerous isolated dykes. The gabbroic cumulates consist of olivine gabbro, gabbro and gabbronorite. The major and trace element geochemistry of the mafic cumulate rocks suggests that the primary magma was compositionally similar to those observed in modern island-arc tholeiitic sequences. The isolated dykes are exclusively basaltic in composition and display geochemically two distinct subgroups: Group I is represented by high TiO_2 (.87–1.47 wt.%) and other incompatible elements, whereas Group II is characterized by low TiO_2 (.36–.66 wt.%) and other incompatible elements. The Group I isolated diabase dykes have flat to slightly LREE-depleted profiles (La/Yb_N = .32–.79), whereas the Group II isolated diabase dykes are more depleted in general and have a LREE-depleted character (La/Yb_N = .19–.49). This suggests that the isolated dykes were derived from an island arc tholeiitic magma (Nb/Y = .02–.05) with different degrees of partial melting (Group II > Group I) and relatively high oxygen fugacity in intra-oceanic subduction zone. The ophiolitic rocks in the study area may well be compared with the Divriği ophiolite to the southeast. All the evidence suggests that the isolated dykes in the Tecer Mountain area differ from the alkaline isolated dykes cutting the Divriği ophiolite. Since the late stage dykes (~76 Ma) in the Divriği area are alkaline, the tholeiitic isolated dykes in the present study should have been emplaced prior to the alkaline dykes during Late Cretaceous SSZ-spreading (~90 Ma) within the Inner Tauride Ocean.

ARTICLE HISTORY
Received 25 December 2016
Accepted 23 July 2017

KEYWORDS
Inner Tauride suture; ophiolite; mélange; isolated dykes; tholeiite

1. Introduction

The Tauride Mountain Range in southern Turkey includes a number of Late Cretaceous ophiolites, mélanges and related metamorphic rocks. From west to east, these are the Lycian nappes, the Tekirova (Antalya) ophiolite, the Beyşehir-Hoyran nappes, the Mersin ophiolite, the Alihoca ophiolite, the Pozantı-Karsantı ophiolite, the Pınarbaşı ophiolite and the Divriği ophiolite (Figure 1). Situated above the Tauride passive continental margin, they mainly exhibit three tectono-stratigraphic/magmatic units such as, from bottom to top, ophiolitic mélange, sub-ophiolitic metamorphic sole and dismembered oceanic lithospheric section. Except for the melange unit, the mantle tectonites, cumulates and metamorphic soles are intruded mostly by isolated microgabbro-diabase dykes and, to a lesser extent, pyroxenite dykes. The isolated dykes are not deformed, indicating that they were emplaced shortly after formation of the metamorphic soles, but they do not extend into the underlying mélanges and platform carbonates. The ophiolites along the Tauride belt were formed in supra-subduction zone (SSZ) settings and emplaced in the Late Cretaceous from different oceanic basins (Andrew & Robertson, 2002; Bağcı, Parlak, & Höck, 2006; Çelik, 2007; Çelik & Chiaradia, 2008; Çelik & Delaloye, 2003; Collins & Robertson, 1997; Collıns & Robertson, 1998; Dilek, Thy, Hacker, & Grundvig, 1999; Dilek & Whitney, 1997; Elitok, 2001; Elitok & Drüppel, 2008; Parlak & Delaloye, 1996; Parlak, Delaloye, & Bíngöl, 1996; Parlak, Höck, & Delaloye, 2000, 2002; Parlak & Robertson, 2004; Parlak, Yılmaz, & Boztuğ, 2006; Robertson, 2002; Robertson, Parlak, & Ustaomer, 2012; Robertson & Woodcock, 1981a, 1981b, 1981c, 1982; Robertson, Parlak, Metin, et al., 2013; Vergili & Parlak, 2005). The metamorphic soles beneath the ophiolites along the Tauride belt yield well-constrained Late Cretaceous $^{40}Ar/^{39}Ar$ plateau ages (Çelik, Delaloye, & Feraud, 2006; Dilek et al., 1999; Parlak & Delaloye, 1999).

CONTACT Osman Parlak parlak@cukurova.edu.tr
Supplemental data for this article can be accessed here [https://doi.org/10.1080/09853111.2017.1359773].

© 2017 The Author(s). Published by Informa UK Limited, trading as Taylor & Francis Group.
This is an Open Access article distributed under the terms of the Creative Commons Attribution License (http://creativecommons.org/licenses/by/4.0/), which permits unrestricted use, distribution, and reproduction in any medium, provided the original work is properly cited.

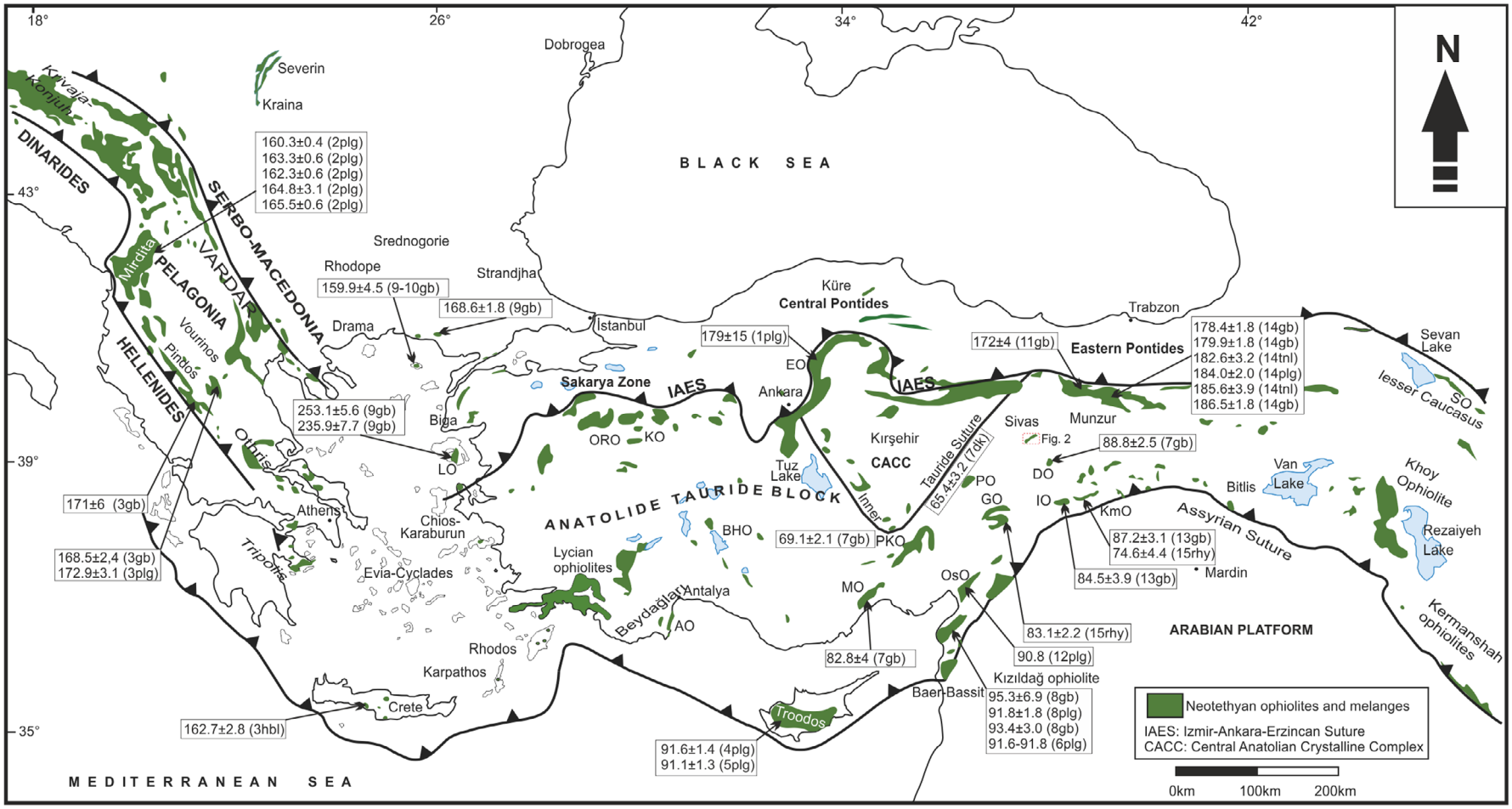


Figure 1. U-Pb ages of Tethyan ophiolites in Turkey and surrounding areas. Data are from (1) Dilek and Thy (2006), (2) Dilek, Furnes, and Shallo (2008), (3) Liati, Gebauer, and Fanning (2004), (4) Mukasa and Ludden (1987), (5) Konstantinou, Wirth, and Vervoort (2007), (6) Dilek and Thy (2009), (7) Parlak, Karaoğlan, Rızaoğlu, Klötzli, et al. (2013), (8) Karaoğlan, Parlak, Klötzlı, Thönı, and Koller (2013), (9) Koglin (2008), (10) Koglin, Kostopoulos, and Reischmann (2009), (11) Topuz et al. (2012), (12) Sarıfakıoğlu, Dilek, and Uysal (2012), (13) Karaoğlan, Parlak, Klötzli, Thöni, and Koller (2012), (14) Robertson, Parlak, Ustaömer, et al. (2013), (15) Karaoğlan, Parlak, Klötzli, Koller, and Rızaoğlu (2013).

Abbreviations: LO: Lesvos Ophiolite, AO: Antalya Ophiolite, BHO: Beyşehir-Hoyran Ophiolite, ORO: Orhaneli Ophiolite, KO: Kınık Ophiolite, EO: Eldivan Ophiolite, MO: Mersin Ophiolite, PKO: Pozanti-Karsanti Ophiolite; OsO: Osmaniye Ophiolite, GO: Göksun Ophiolite, PO: Pinarbaşi Ophiolite, IO: Ispendere Ophiolite, DO: Divriği Ophiolite, KmO: Kömürhan Ophiolite, SO: Sevan Ophiolite; plg: plagiogranite, gb: gabbro, dk: dyke, tnl: tonalite, rhy: rhyolite [Map modified after Dilek and Flower (2003) and Çelik et al. (2011)].

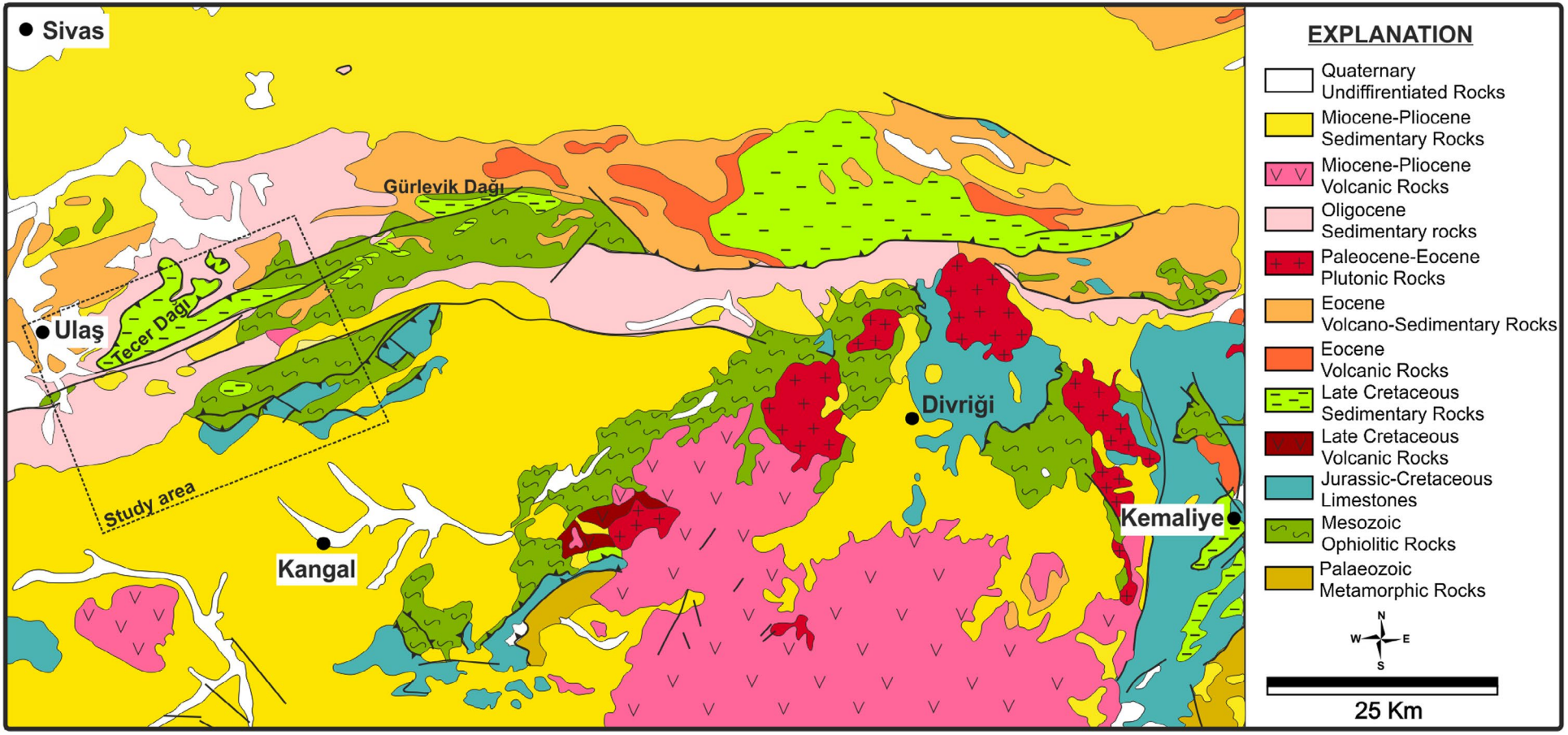


Figure 2. 1/500.000 scale geological map of the Ulaş-Kangal-Divriği (Sivas) regions, showing the distribution of the Tauride platform, ophiolites, granitoids and cover sediments (from MTA, 2002).

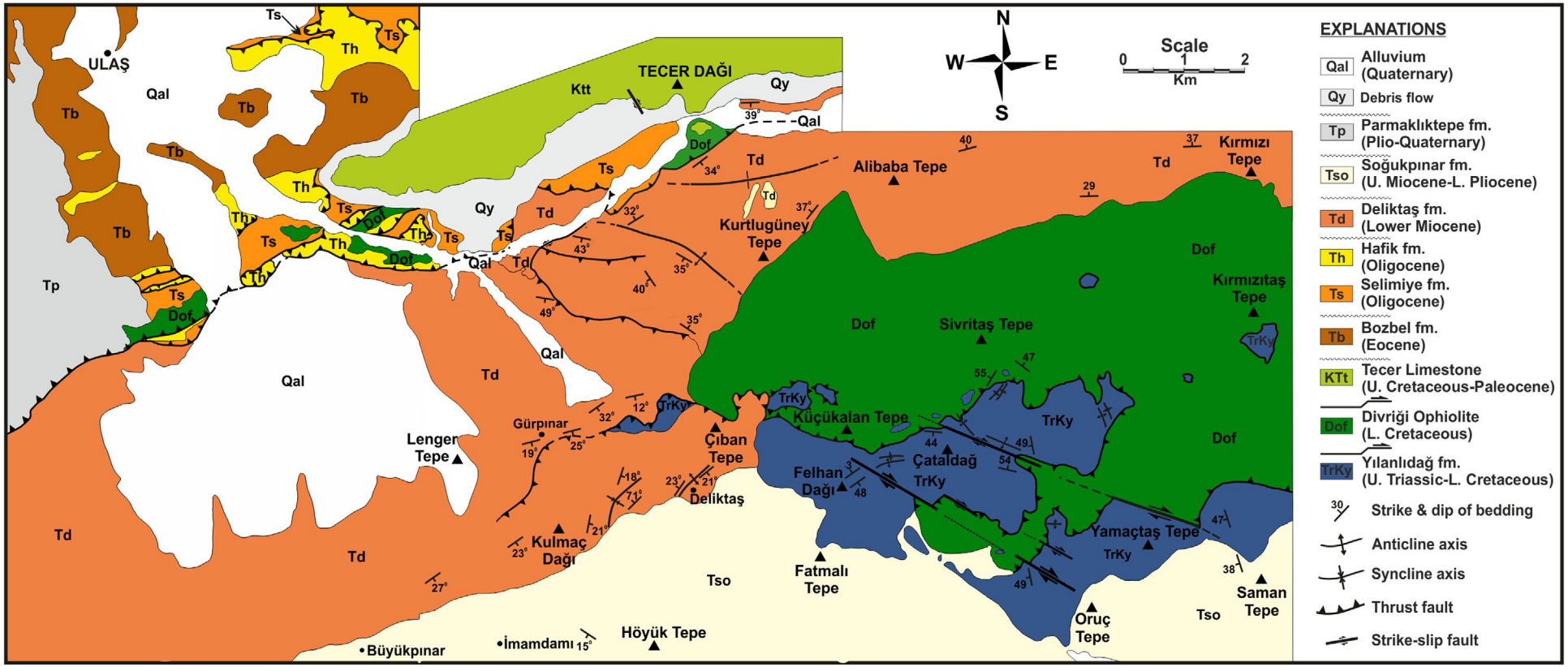


Figure 3. Geological map of the southern margin of the Sivas basin in the Tecer area (Kavak, 2010). Source: Kaan Şevki Kavak.

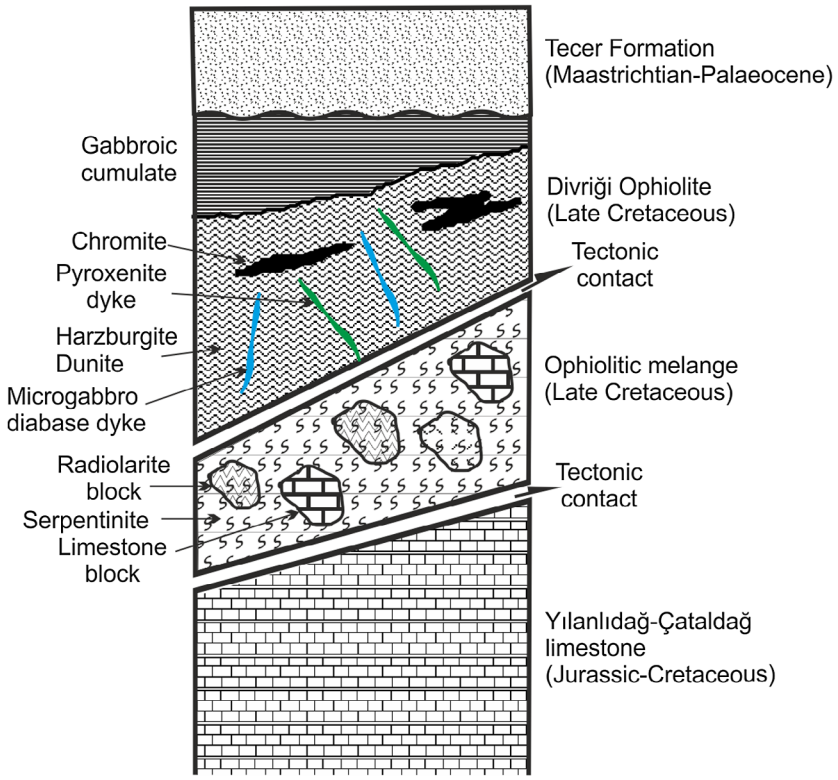


Figure 4. The tectonostratigraphy of the units around the southern margin of the Sivas basin.

The Late Cretaceous Divriği (Sivas) ophiolite, tectonically resting on top of the Munzur limestone (Tauride platform), is located between Çetinkaya and Divriği (Sivas) towns in east-central Anatolia and consists of, from bottom to top, an ophiolitic melange, metamorphic sole and remnants of oceanic lithosphere (mantle tectonites, cumulates, isotropic gabbro and sheeted dykes) (Parlak et al., 2006; Yılmaz, Arıkal, & Yılmaz, 2001). The Divriği ophiolite formed in a suprasubduction zone setting above a north-dipping intra-oceanic subduction zone within the Inner Tauride Ocean (Parlak et al., 2006). The crystallization age of the SSZ-type oceanic crust was determined as 88.8 ± 2.5 Ma by LA-MC-ICP-MS U-Pb zircon on the gabbroic cumulates (Parlak, Karaoğlan, Rızaoğlu, Klötzli, et al., 2013). The alkaline to tholeiitic amphibolites from the metamorphic sole yielded similar ^{40}Ar–^{39}Ar cooling ages (89.65 ± .97 and 87.49 ± .48 Ma) that can compare well with the age of the overlying SSZ-type crust (Parlak, Karaoğlan, Rızaoğlu, Klötzli, et al., 2013). The isolated dykes intruding the Divriği ophiolite are alkaline and were interpreted to have been derived as a result of slab break-off (Parlak et al., 2006) in the late Cretaceous (75.9 ± .30 Ma) before the final emplacement (Parlak, Karaoğlan, Rızaoğlu, Klötzli, et al., 2013).

In the Tecer Mountain area along the southern margin of the Sivas basin, the ophiolite-related rocks in tectonic contact with the Tauride platform crop out beneath the Upper Cretaceous-Palaeocene Tecer limestone along a NE-SW-trending tectonic zone that is parallel to the main Divriği ophiolite further to the southeast (Figure 2). The contact relation of the two zones in the study area is obscured by extensive Oligo-Miocene sedimentary cover. The study area includes mainly the Tauride platform, the melange and ophiolitic rocks. The ophiolitic rocks are dominated by variably serpentinized mantle harzburgite and gabbroic cumulates. The mantle tectonites are intruded by a number of isolated dykes, mainly microgabbro to diabase and, less commonly, pyroxenite. Parlak et al. (2006) recorded that the isolated microgabbro to diabase dykes in Divriği (Sivas) ophiolite were derived from an alkaline magma, derived from late-stage melts with enriched compositions. Such melts with enriched compositions would be generated along local fractures or tears in the subducting plate or large-scale break-off. The geochemistry of the isolated dykes cutting the mantle tectonites in the Tecer Mountain area has a tectonic significance, and it was considered important to test whether they are similar to the isolated dykes in Divriği ophiolite or different in origin.

The root zone of the ophiolites in the Eastern Taurides and on the top of the Niğde-Kırşehir microcontinent has been debatable. According to some workers the ophiolites were derived from the Inner Tauride Ocean between, located between Niğde-Kırşehir microcontinent and the Tauride-Anatolide continent (Dilek et al., 1999; Okay & Tüysüz, 1999; Pourteau, Candan, & Oberhänsli, 2010; Robertson, Parlak, & Ustaömer, 2009; Robertson, Parlak, Metin, et al., 2013). However number of authors have preferred to correlate all of these ophiolites with the Northern Neotethys (Göncüoğlu, Dirik, & Kozlu, 1996–1997; van Hinsbergen et al., 2016).



Figure 5. Field views of ophiolitic rocks from the study area. (a) Tectonic contact between the Tauride platform and the ophiolites, (b) radiolites and mafic rocks in the melange, (c) isolated dykes cutting the mantle tectonites, (d) serpentinized mantle harzburgite, (e) cumulate gabbros and (f) the contact between the ophiolite and the Tecer limestone. Source: Osman Parlak.

Our objectives here are to (a) present major- and trace-element chemistry of the isolated diabase and pyroxenite dykes, and cumulate gabbro from the Tecer Mountain area, (b) correlate their origin with the Divriği (Sivas) ophiolite as well as the other Tauride ophiolites in the region and (c) discuss their tectonic significance for the magmatic evolution of the Inner Tauride Ocean.

2. Field relations & petrography

The study area is located south of the Tecer Mountains where the ophiolitic units are interpreted to have been derived from the Inner Tauride Ocean (Gökten, 1993; Görür, Oktay, Seymen, & Şengör, 1984; Robertson, Parlak, Metin, et al., 2013). Tectono-stratigraphic and magmatic units ranging in age from Mesozoic to Cenozoic crop out, (Figures 3 and 4) while the basement is represented by the Upper Triassic-Lower Cretaceous Yılanlıdağ limestone of the Tauride carbonate platform (Munzur limestone) which is tectonically overlain by ophiolitic rocks in the region (Figure 4) with a mélange unit at the contact. This melange includes blocks of basalt and pelagic limestone set in an ophiolite-derived matrix (Robertson, Parlak, Metin, et al., 2013). In some places, towards the contact with the Tauride platform in the Yılanlıdağ area, olistoliths of limestone and radiolarite are set in sheared serpentinites (Figure 5). The melange unit is overlain by mantle tectonites cut by isolated diabase and pyroxenite dykes at different structural levels (Figure 5). A minor amount of cumulate gabbro is locally exposed (Figure 5). Actively mined chromitite occurences within the mantle tectonites form a considerable economic resource in the region. A complete ophiolite suite southeast of the present study area, called the Divriği ophiolite (Yılmaz et al., 2001), was interpreted to have been derived from the same (i.e. Inner Tauride) oceanic basin (Parlak et al., 2006; Robertson, Parlak, Metin, et al., 2013). The mantle tectonites are dominated by

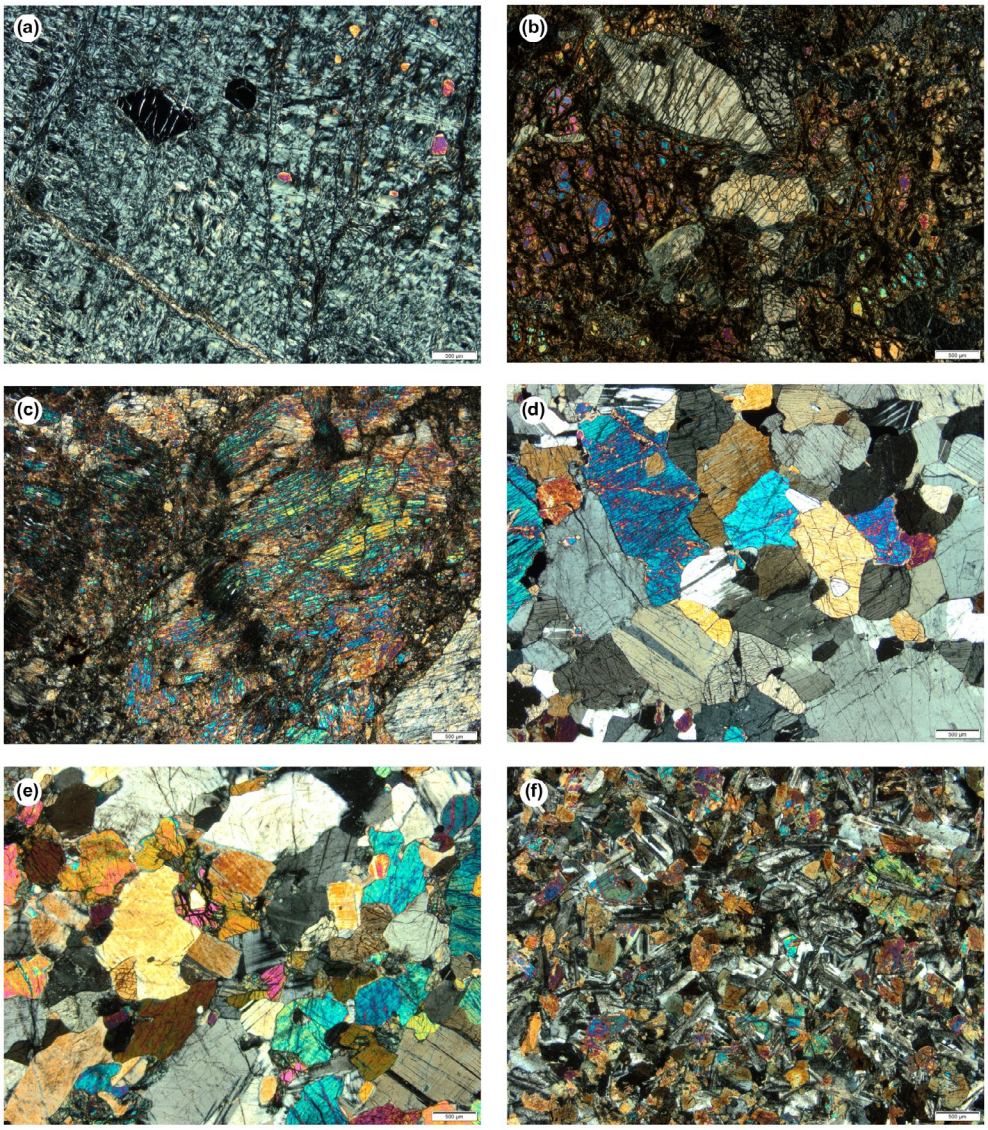


Figure 6. Thin-section views of the ophiolitic rocks in the study area. (a) Serpentinite, (b) harzburgite, (c) pyroxenite dyke, (d) gabbro, (e) olivine gabbro and (f) diabase dyke.

serpentinites, serpentinized harzburgites and contain, to a lesser extent, dunites (Figure 6(a) and (b)). The serpentinite is widely altered to listwaenite. The serpentinized harzburgites display porphyroclastic to mesh textures and consist of olivine (70–85 vol.%), orthopyroxene (15–20 vol.%), clinopyroxene (<3 vol.%), and chromian spinel (1–1.5 vol.%). Dunites consist of olivine grains that are divided into numerous small grains by a serpentine mesh texture. The isolated dykes cutting the mantle tectonites are quite common and are typically microgabbro-diabase, microdiorites and pyroxenite. The dykes have sharp contacts with the host rocks and lack chilled margins, suggesting that the host rocks were still hot at the time of dyke emplacement (Figure 6). The pyroxenite dykes have a granular texture and are from 10 to 60 cm thick (Figure 6(c)). They are made anhedral clinopyroxene (85–90 vol.%), orthopyroxene (7–8 vol.%) and opaque minerals. The microgabbro-diabase dykes, 50 cm to 2 m thick, exhibit a subophitic texture (Figure 6(f)) and contain plagioclase (50–55 vol.%) and clinopyroxene (20–30 vol.%). The clinopyroxenes are partly replaced by amphibole. The microdiorites have microgranular to intergranular textures and are characterized by plagioclase (55–60 vol.%), amphiboles (25–30 vol.%) and pyroxenes (5–10 vol.%). Epidote and chlorite are secondary phases. Some of the amphiboles have been transformed from pyroxenes. The gabbro, gabbronorite and olivine gabbro mafic cumulate blocks (Figure 6(d) and (e)) are very fresh and exhibit a banded cumulate texture. The gabbros consist mainly of plagioclase (60–70 vol.%), clinopyroxene (15–20 vol.%) and orthopyroxene (2–3 vol.%). The gabbronorite comprises plagioclase (55–65 vol.%), orthopyroxene (15–20 vol.%) and clinopyroxene (20–25 vol.%). The olivine gabbro contains cumulus olivine (20–25 vol.%), plagioclase (~60 vol.%), clinopyroxene (15–20 vol.%) and orthopyroxene (1–2 vol.%). The ophiolite-related rocks south of the Tecer Mountains along the southern margin of the Sivas basin are interpreted as part of the Divriği ophiolite found more to the south-southeast (Figure 2).

Table 1. Major and trace element contents of the isolated dykes in the study area.

	IAT-type isolated dykes												Low-Ti isolated dykes				
Sample	TO-1	TO-3	TO-5	TO-6	TO-12	TO-11	TO-14	TO-16	TO-19	TO-21	TO-23	TO-24	TO-22	TO-25	TO-26	TO-27	TO-28
SiO_2	46.20	47.87	44.71	50.76	47.02	45.65	44.05	44.13	50.25	46.19	46.32	42.44	43.95	51.08	50.23	47.21	51.27
TiO_2	1.47	1.05	1.23	1.11	.87	.94	1.31	1.03	.90	1.45	1.18	1.22	.42	.48	.37	.66	.36
Al_2O_3	15.46	15.77	17.97	14.86	15.14	14.95	16.76	15.87	16.02	16.00	15.67	16.88	16.57	15.87	13.04	16.93	14.53
FeO*	12.86	9.57	9.22	10.62	8.92	9.49	10.63	12.71	9.44	11.79	12.14	9.13	9.06	9.42	9.55	10.70	9.01
MgO	7.39	7.42	6.91	6.12	7.05	6.61	6.98	4.57	6.87	7.56	7.51	8.30	8.68	7.22	11.25	6.74	8.40
CaO	10.11	9.77	14.76	7.46	10.85	11.86	13.56	7.78	9.51	11.22	11.57	16.68	15.71	9.59	9.16	8.15	9.45
Na_2O	2.99	4.47	1.11	4.52	4.22	4.62	.71	7.16	4.21	3.03	2.61	1.26	1.29	3.17	2.47	4.51	3.21
K_2O	.39	.14	<.01	.07	.41	.47	.63	.24	.27	.23	.40	.16	.23	.98	.82	.15	.50
P_2O_5	.12	.08	.09	.06	.07	.09	.14	.10	.08	.14	.09	.13	.01	.02	.03	.05	.05
MnO	.22	.15	.12	.17	.14	.15	.13	.18	.15	.18	.18	.13	.14	.15	.15	.15	.14
Cr_2O_3	<.002	.03	.01	.01	.02	.02	.02	.00	.02	.02	.01	.02	.02	.01	.09	.01	.04
LOI	2.60	3.50	3.60	4.00	5.00	4.90	4.80	6.00	2.00	1.90	2.00	3.30	3.00	1.80	2.50	4.50	2.70
Sum	99.77	99.77	99.79	99.78	99.72	99.80	99.69	99.79	99.76	99.69	99.70	99.67	99.12	99.77	99.70	99.74	99.73
Ba	34	27	9	43	151	15	35	23	25	20	70	84	410	44	53	22	61
Co	37.9	41.3	51.8	54.4	44.9	38.2	55.3	47.9	45.1	73.7	54.7	53.2	57.1	48.2	54.6	50.6	47.4
Cs	3.2	.4	<.1	.2	7.2	2.2	1.5	.2	<.1	.7	.2	.1	.2	.4	.3	.9	.2
Ga	16.2	14	15.2	12.6	12.4	13.5	15.4	17.6	15.3	16.2	16.2	14.5	12.6	14.4	10.4	15.9	12.7
Hf	2	1.8	2	1.7	1.3	1.7	2.4	1.8	1.4	1.6	1.4	.9	.4	.6	.5	.7	.4
Nb	1.4	1.1	.9	.6	.8	.7	1.1	.8	.8	1.3	1	.9	.2	.5	.4	.6	.3
Rb	7	3	.5	1.4	7.7	18.9	9.7	3.6	2.9	1.7	3.8	2.2	1.9	12.2	9	2.1	5.8
Sr	116.1	282.6	266.1	281.5	400.7	107	607.9	102.2	130.8	206.2	375.6	754.8	5248.7	185	268	167.6	331.7
Ta	.2	<.1	<.1	<.1	<.1	<.1	<.1	<.1	<.1	.4	.1	<.1	<.1	<.1	<.1	<.1	<.1
Th	<.2	.4	.5	<.2	.4	.2	.4	.4	.2	.4	.2	<.2	<.2	<.2	<.2	<.2	.2
U	<.1	<.1	.1	<.1	<.1	.1	.2	.1	<.1	<.1	<.1	<.1	<.1	<.1	<.1	.1	<.1
V	418	265	357	302	252	249	352	440	278	349	403	383	320	285	263	387	265
Zr	50.2	59.2	63.2	57.9	42.4	45.3	73.2	44.2	51.5	47.2	34.2	20.5	7.8	18.6	13	18.7	11.5
Y	30.2	21	25.1	23.2	19.2	21.2	30.3	24.6	22.1	31.8	25	30.5	13	13.1	10.2	14.1	10.9
Pb	.5	.3	.6	.3	.2	.4	<.1	.6	.2	.3	.5	.3	.2	.5	.4	.5	.4
Ni	12.7	30.4	14.3	20.4	30.6	25.4	19.2	18.2	30.1	28.2	62.7	43.2	28.3	17.6	46.9	25.8	55.6
Sc	38.00	37.00	41.00	36.00	37.00	36.00	40.00	41.00	37.00	45.00	45.00	47.00	47.00	40.00	43.00	43.00	41.00
Zr/Ti	.006	.009	.009	.009	.008	.008	.009	.007	.010	.005	.005	.003	.003	.006	.006	.005	.005
Nb/Y	.046	.052	.036	.026	.042	.033	.036	.033	.036	.041	.040	.030	.015	.038	.039	.043	.028
Ti/Y	291.810	299.750	293.779	286.830	271.648	265.816	259.190	251.010	244.140	273.357	282.964	239.800	193.685	219.664	217.466	280.617	198.000
Ce/Y	.225	.338	.287	.263	.281	.307	.290	.199	.299	.277	.292	.167	.108	.221	.157	.163	.147
Zr/Nb	35.857	53.818	70.222	96.500	53.000	64.714	66.545	55.250	64.375	36.308	34.200	22.778	39.000	37.200	32.500	31.167	38.333
Sm/Yb	.905	1.066	.882	.920	.874	.886	.930	.743	.884	.966	.903	.833	.586	.638	.569	.607	.438
Ce/Sm	2.290	2.922	2.927	2.531	3.121	3.218	3.014	2.487	3.204	2.794	3.147	1.932	1.573	2.843	2.424	2.323	2.857
Nb/Th	–	2.750	1.800	–	2.000	3.500	2.750	2.000	4.000	3.250	5.000	–	–	–	–	–	1.500

Note: Total Fe is expressed as FeO*; < means below detection limit.

Table 2. REE contents of the isolated dykes in the study area.

	IAT-type isolated dykes												Low-Ti isolated dykes				
Sample	TO-1	TO-3	TO-5	TO-6	TO-12	TO-11	TO-14	TO-16	TO-19	TO-21	TO-23	TO-24	TO-22	TO-25	TO-26	TO-27	TO-28
La	2	2.5	2.5	2	1.9	2.1	2.8	1.7	2.4	2.4	2.3	1.4	.4	1.1	.6	.9	.7
Ce	6.8	7.1	7.2	6.1	5.4	6.5	8.8	4.9	6.6	8.8	7.3	5.1	1.4	2.9	1.6	2.3	1.6
Pr	1.41	1.32	1.28	1.15	.96	1.11	1.53	.89	1.14	1.61	1.27	1.05	.29	.44	.27	.42	.24
Nd	7.5	7.7	6.9	6.9	5	6.4	9.6	5	6.5	9.4	8	5.9	1.7	2.5	1.7	2.4	1.3
Sm	2.97	2.43	2.46	2.41	1.73	2.02	2.92	1.97	2.06	3.15	2.32	2.64	.89	1.02	.66	.99	.56
Eu	1.12	.93	1	.89	.79	.83	1.34	.79	.84	1.17	.96	1.16	.33	.39	.3	.35	.27
Gd	4.27	3.23	3.6	3.38	2.6	2.83	4	2.87	3.02	4.35	3.42	3.85	1.4	1.54	1.08	1.59	1.11
Tb	.82	.61	.67	.64	.53	.61	.82	.62	.61	.86	.68	.81	.31	.32	.24	.33	.25
Dy	5.36	3.85	4.33	4.21	3.2	3.6	5.33	4.03	3.73	5.33	4.2	5.01	2.07	2.12	1.51	2.1	1.67
Ho	1.17	.85	.99	.9	.68	.78	1.06	.84	.77	1.14	.88	1.08	.47	.46	.34	.48	.41
Er	3.2	2.41	2.78	2.67	2.1	2.22	3.21	2.6	2.36	3.35	2.6	3.18	1.39	1.51	1.18	1.57	1.24
Tm	.5	.36	.43	.4	.32	.36	.5	.41	.37	.5	.4	.48	.21	.25	.16	.24	.19
Yb	3.28	2.28	2.79	2.62	1.98	2.28	3.14	2.65	2.33	3.26	2.57	3.17	1.52	1.6	1.16	1.63	1.28
Lu	.5	.35	.42	.39	.3	.34	.46	.42	.33	.45	.38	.43	.22	.22	.18	.24	.2

Table 3. Major, trace and rare earth element contents of the cumulate gabbros and pyroxenite dyke in the study area.

	Cumulate gabbros				Pyroxenite dyke
Sample	TO-7	TO-8	TO-10	TO-18	TO-17
SiO_2	41.62	45.07	46.48	46.43	49.97
TiO_2	<.01	.10	.22	.12	.05
Al_2O_3	26.61	14.67	16.87	20.82	1.14
FeO*	2.48	5.38	7.08	8.77	3.98
MgO	9.38	15.84	10.83	9.46	20.37
CaO	13.79	14.01	15.95	12.59	20.04
Na_2O	.66	.52	1.15	.57	.05
K_2O	<.01	<.01	.04	.07	<.01
P_2O_5	<.01	<.01	<.01	.02	.03
MnO	.03	.09	.12	.15	.11
Cr_2O_3	.080	.185	.072	.011	.415
LOI	5.1	3.8	.9	.7	3.4
Sum	99.83	99.71	99.76	99.75	99.64
Ba	9	<1	5	2	6
Co	30.3	57.6	55.3	68.1	48.6
Cs	<.1	<.1	<.1	<.1	<.1
Ga	9.0	6.9	10.6	12.1	1.5
Hf	<.1	<.1	<.1	<.1	<.1
Nb	<.1	<.1	<.1	<.1	<.1
Rb	.5	.3	.4	.8	<.1
Sr	130.7	56.0	80.7	97.1	5.2
Ta	<.1	<.1	<.1	<.1	<.1
Th	<.2	<.2	<.2	<.2	<.2
U	<.1	<.1	<.1	<.1	<.1
V	12	94	154	141	124
Zr	<.1	1.0	5.5	.4	.9
Y	.2	2.9	6.2	1.2	.8
Pb	.3	.1	.1	<.1	<.1
Ni	379.3	289.0	92.0	9.3	134.5
Sc	2	35	45	30	55
La	<.1	.1	.5	.3	.1
Ce	<.1	.3	.8	.2	.2
Pr	<.02	.06	.18	.03	.03
Nd	<.3	.5	1.2	<.3	<.3
Sm	<.05	.21	.50	<.05	<.05
Eu	.05	.14	.26	.09	.03
Gd	<.05	.38	.83	.10	.08
Tb	<.01	.08	.17	.03	.03
Dy	<.05	.52	1.09	.22	.19
Ho	<.02	.12	.23	.04	.03
Er	<.03	.33	.68	.14	.13
Tm	<.01	.05	.10	.02	.01
Yb	<.05	.27	.65	.19	.10
Lu	<.01	.05	.09	.02	.01

Note: Total Fe is expressed as FeO*; < means below detection limit.

The oldest unit resting unconformably above the ophiolitic unit is the Upper Cretaceous-Palaeocene Tecer formation, composed of a shallow marine mixed carbonate-clastic facies (Atabey & Aktimur, 1997; İnan & İnan, 1987; Robertson, Parlak, Metin, et al., 2013). In some places, the contact is tectonic (Figure 2). The Tecer

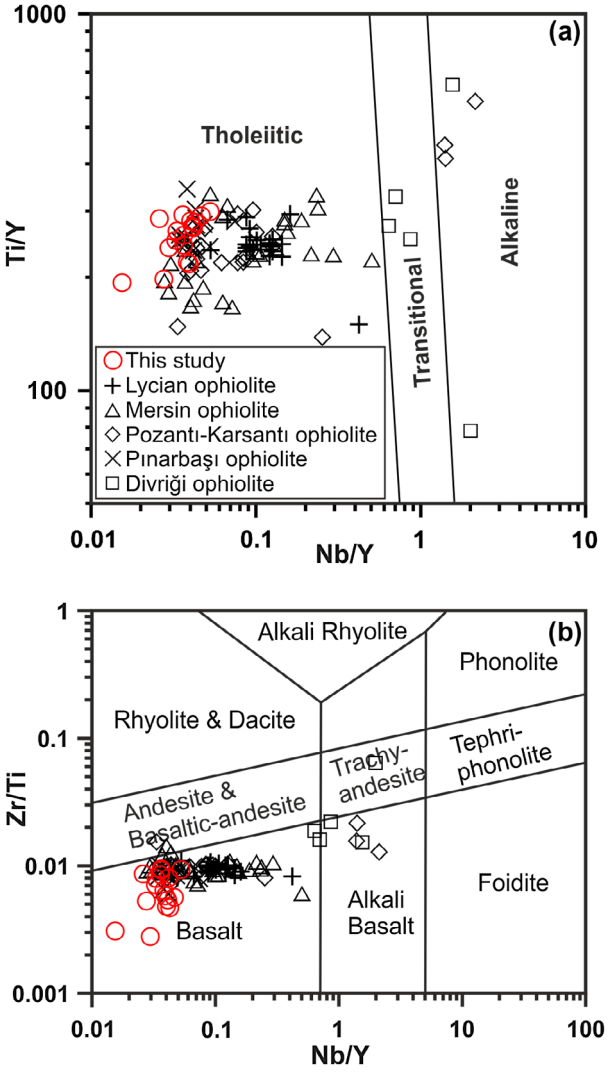


Figure 7. (a) Ti/Y vs. Nb/Y (after Pearce, 1982) and (b) Zr/Ti vs. Nb/Y (after Pearce, 1996) diagrams for the isolated dykes from the study area and other Tauride ophiolites (Çelik, 2007, 2008; Çelik & Chiaradia, 2008; Çelik & Delaloye, 2003; Parlak et al., 1995, 2006; Parlak & Delaloye, 1996; Vergili & Parlak, 2005).

formation, in turn, is unconformably overlain by continental to shallow marine sediments ranging in age from Oligocene to Plio-Quaternary (Figure 3).

3. Analytical method

To determine the geochemical and petrological characteristics of the isolated diabase and pyroxenite dykes and cumulate gabbro from the ophiolitic rocks at the southern edge of the Sivas basin, south of the Tecer Mountains, a total of 22 samples were analyzed at Acme Analytical Laboratories Ltd (Canada) for whole rock major, trace and rare earth elements. Major element contents were determined from a $LiBO_2$ fusion by ICP-ES (Inductively coupled plasma-emission spectrometry) by using 5 grams of sample pulp. Trace element contents were determined from a $LiBO_2$ fusion by ICP-MS (Inductively coupled plasma-mass spectrometry) by using 5 grams of sample pulp. The results of the analyses are presented in Tables 1–3.

4. Geochemistry

Major and trace element concentrations in the isolated dykes are presented in Table 1 and 2. The isolated dykes display variable loss on ignition (LOI) values between 1.8 and 6% (Table 1) and this wide variation is a crude measure of their degree of alteration and reflects the proportion of secondary hydrated aqueous or carbonate phases (Rollinson, 1993). As mobility of major and trace elements (LIL-large ion lithophiles) has been noted due to alteration after formation of a rock (Hart, Erlank, & Kable, 1974; Humphris & Thompson, 1978; Thompson, 1991), rare earth elements (REE) and HFS (high field strength) elements which are resistant to mobility caused by alteration have been used (Floyd & Winchester, 1978; Pearce & Cann, 1973).

The Nb/Y vs. Ti/Y ratio diagram discriminates between the tholeiitic and alkaline magmas (Pearce, 1982). The isolated dyke samples from the southern margin of the Sivas basin exhibit Ti/Y (194–300) and Nb/Y (.02–.05) ratios, suggesting derivation from a tholeiitic magma (Figure 7(a)). Isolated dykes intruding the Tauride ophiolites at different structural levels (i.e. Lycian, Mersin, Pozantı-Karsantı, Pınarbaşı and Divriği) are also plotted for comparison. Those from the different Tauride ophiolites were generally derived from a tholeiitic magma (Çelik, 2007, 2008; Çelik & Chiaradia, 2008; Çelik & Delaloye, 2003; Parlak, 2000; Parlak & Delaloye, 1996; Parlak, Delaloye, & Bingöl, 1995; Vergili & Parlak, 2005), although alkaline magma-derived isolated dykes have also been reported (Çelik, 2007; Parlak et al., 2006). The isolated dykes from the study area are exclusively represented by basaltic rock types based on their Nb/Y (.02–.05) and Zr/Ti (.003–.01) ratios (Pearce, 1996) (Figure 7(b)).

All the interelement relations and immobile trace element contents suggest two geochemically distinct subgroups, both derived from tholeiitic magma, in the isolated diabase dykes cutting the ophiolites in the Tecer Mountain area (Sivas). The first geochemical group contains higher TiO_2 (.87–1.47 wt.%), Zr (20.5–73.2 ppm), Y (19.2–31.8 ppm), Hf (.9–2.4 ppm) and Nb (.6–1.4 ppm) and low MgO (4.57–8.30 wt.%) than the second geochemical group, which has low TiO_2 (.36–.66 wt.%), Zr (7.8–18.7 ppm), Y (10.2–14.1 ppm), Hf (.4–.7 ppm) and Nb (.2–.6 ppm) and high MgO (6.74–11.25 wt.%) (Table 1). Immobile trace element variations (Zr vs. Ti, Zr vs. Y and Zr vs. V) as well as FeO* (Figure 8) display generally a positive correlation and similar trend to the tholeiitic isolated dykes reported from the other Tauride ophiolites. This evidence is consistent with crystallization of olivine, clinopyroxene and plagioclase (Pearce, 1982; Pearce & Norry, 1979). Decreasing MgO contents relative to Zr suggest that olivine was an important phase during primary fractionation (Figure 8). The inter-element relations based on immobile elements suggest that the tholeiitic isolated dykes from the study area and the other parts of the Tauride ophiolites show similar geochemical

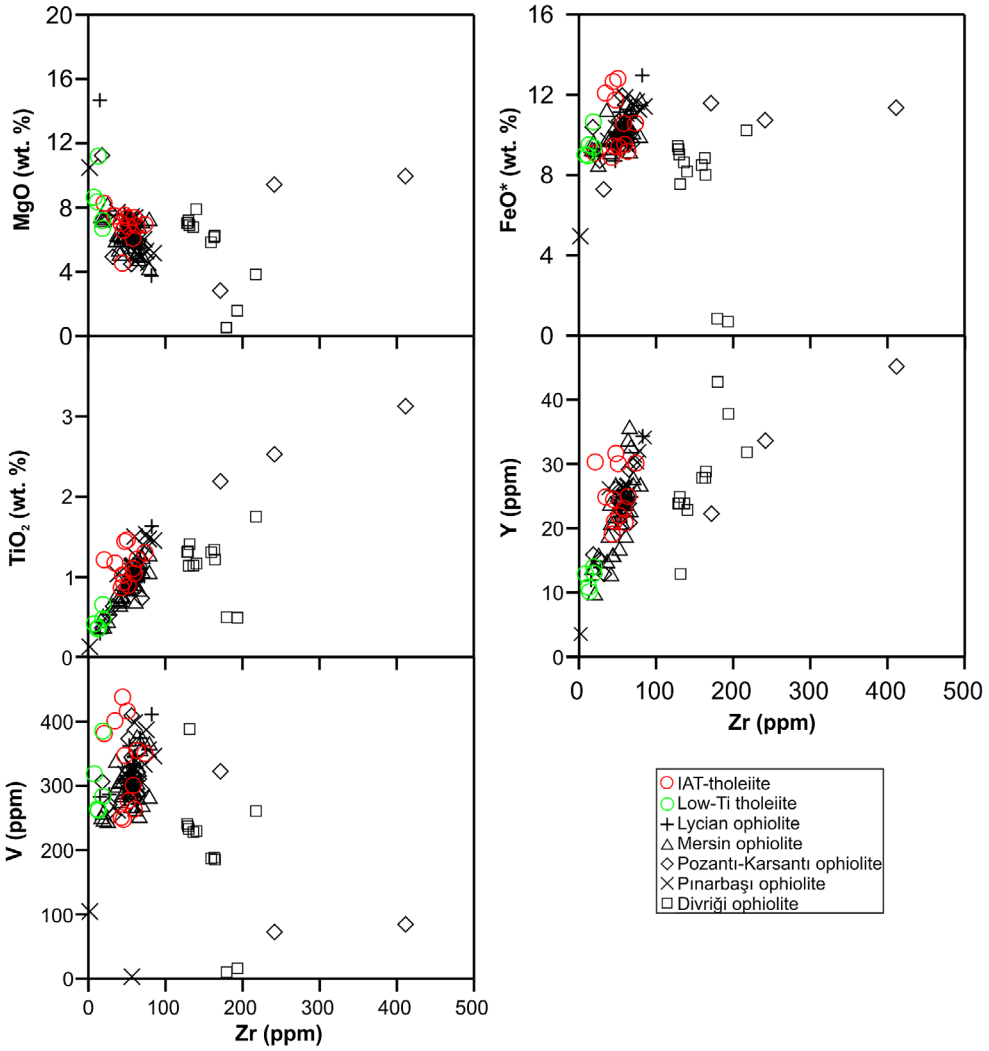


Figure 8. Variation of selected major and trace elements for the isolated dykes in the study area and other Tauride ophiolites. Data for the isolated dykes of the Tauride ophiolites are the same as in Figure 7.

features, consistent with co-magmatic relationships, whereas the alkaline dyke rocks (Zr > 100 ppm) from the Pozantı-Karsantı and Divriği ophiolites exhibit a different evolutionary trend (Figure 8).

In order to characterize the degree of partial melting of the source from which the isolated dykes were derived, a Ce/Y vs. Zr/Nb plot of elements with different degrees of incompatibility is used in Figure 9(a). Partial melting is lowest where Ce/Y values are the highest and increases with increasing Zr/Nb values. In the isolated diabase dykes, the Zr/Nb values for Group I (23–96.5) are relatively higher and those of Group II are lower (31.17–39). This indicates that the isolated dykes were derived from the same source (tholeiitic), but with different degrees of partial melting; the Group I dykes with lower degrees of partial melting and the Group II dykes with higher degrees of partial melting (Figure 9(a)). To identify the mantle source for the isolated diabase dykes, Sm/Yb vs. Ce/Sm ratios were plotted together with Ocean Island Basalt (OIB) and Mid-Ocean Ridge Basalt (MORB) compositions (Figure 9(b)). Accordingly, both groups of the isolated diabase dykes have low Sm/Yb (.44–1.07) and Ce/Sm (1.57–3.22) values (Table 2) suggesting their derivation from a more depleted MORB-like mantle source, similar to the tholeiitic isolated diabase dykes cutting ophiolites in the Tauride belt (Figure 9(b)).

Chondrite-normalized rare earth element (REE) profiles for the isolated diabase dykes are given in Figure 10(a). They are illustrated to compare the REE contents of isolated diabase dykes cutting ophiolites in the Tauride belt. Group I isolated diabase dykes have a flat to slightly LREE-depleted profile (La/Yb_N = .32–.79) and overall REE abundances between x6 and x23 chondritic (Figure 10(a)). The Group II isolated diabase dykes are more depleted in nature and have a slightly LREE-depleted profile (La/Yb_N = .19–.49) with an overall REE abundances between ×1.69 and ×9.8 chondritic (Figure 10(a)). Both the Group I and the Group II dykes display similarities to the tholeiitic dykes and the low-Ti dykes of the Tauride ophiolites (Figure 10(a)) and hence typical island arc tholeiites (i.e. Papua New Guinea, Mariana, Solomon Island, Macquarie Island) (Gust & Johnson, 1981; Jakes & Gill, 1970; Stern, 1979). An N-MORB normalized multi-element diagram for the isolated dykes is presented in Figure 10(b). Except

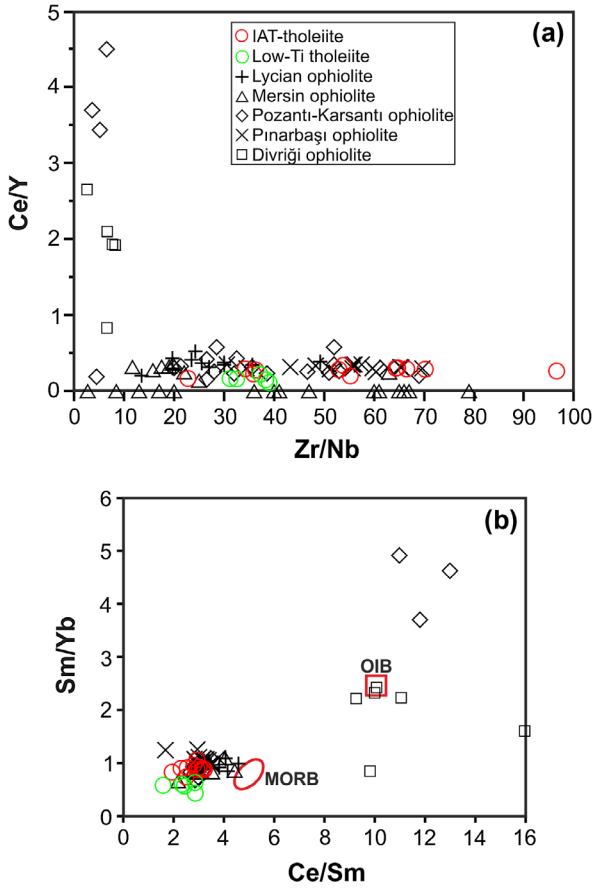


Figure 9. (a) Degree of partial melting (Ce/Y vs. Zr/Nb) and (b) source characteristics (Ce/Sm vs. Sm/Yb) diagrams for the isolated dykes. Data for the isolated dykes of the Tauride ophiolites are the same as in Figure 7.

for the relatively more depleted nature of the Group II isolated dykes compared to Group I, they exhibit similar enrichment/depletion patterns relative to N-MORB (Figure 10(b)): (a) LIL element variations (Rb, Ba, K, Sr etc.), (b) a strong negative Nb anomalies, (c) flat-lying HFS elements. The elevated concentrations of LILE relative to HFSE in subduction zone magmas originate from fluids derived from the subducting slab. These slab-derived fluids carry high concentrations of LILE while the HFSE, most notably Nb, are retained in the slab (Arculus & Powell, 1986; Pearce, 1982; Wallin & Metcalf, 1998; Yogodzinski, Volynets, Koloskov, Seliverstov, & Matvenkov, 1993). Therefore the negative Nb anomaly is clearly intrinsic to the parental magma of the isolated dykes. Th enrichment relative to other incompatible elements is interpreted as indicating a subduction zone component (Pearce, 1983; Wood, Joron, & Treuil, 1979). The negative Nb and positive Th anomalies suggest a suprasubduction zone setting for their genesis. Flat to slightly LREE-depleted patterns and a strong Nb-depletion in MORB-normalized multi-element diagrams for the crustal rocks have been documented in many supra-subduction zone type ophiolites from the Eastern Mediterranean region (Alabaster, Pearce, & Malpas, 1982; Al-Riyami, Robertson, Dixon, & Xenophontos, 2002; Bağcı & Parlak, 2009; Bağcı, Parlak, & Höck, 2008; Beccaluva, Coltorti, Giunta, & Siena, 2004; Beccaluva, Coltorti, Saccani, & Siena, 2005; Dilek & Thy, 2009; Meffre, Aitchison, & Crawford, 1996; Parlak, 1996; Parlak, Höck, Kozlu & Delaloye, 2004; Parlak, Rızaoğlu, Bağcı, Karaoğlan, & Höck, 2009; Parlak et al., 2000; Parlak, Karaoğlan, Rızaoğlu, Nurlu, et al., 2013; Parlak, Çolakoğlu, et al., 2013; Pearce, 2003; Pe-Piper, Tsikouras & Hatzipanagiotou, 2004; Rızaoğlu, Parlak, Höck, & İşler, 2006; Saccani & Photiades, 2005; Vergili & Parlak, 2005; Yalınız, Floyd, & Göncüoğlu, 1996, 2000).

Th-enrichment and Nb-depletion seen in the multi element diagram (Figure 10(b)), are characteristic geochemical features for subduction related settings. On a Nb/Th vs. Y diagram (Jenner, Dunning, Malpas, Brown, & Brace, 1991) to discriminate arc and non-arc settings (Figure 11) the isolated diabase dykes cutting the ophiolite body in the Tecer Mountain area (Sivas) clearly confirm their subduction-related origin (Nb/Th = 1.5–5). Ti/V ratio is used to distinguish Island Arc (≤20), MORB (20–50) and Ocean Island Basalt (>50) (Shervais, 1982). The Ti/V ratio of the Group I dykes range from 14 to 25 and the Group II dykes range from 7.9 to 10.2, suggesting that although the Group I dykes have a minor overlap with MORB values they all formed in a supra-subduction zone setting (Figure 12). The transitional composition from mid-ocean ridge basalt (MORB) to island arc basalt for the Group I dykes may well be attributed to subduction initiation process (Hall, Gurnis, Sdrolias, Lavier, & Müller, 2003). Reagan et al. (2010) described fore-arc basalts (FAB) in the Mariana fore-arc, exhibiting similarities to mid-ocean ridge basalts (MORB) that were derived from more depleted mantle sources with subduction component. These fore-arc basalts (FAB) from the Izu-Bonin-Mariana (IBM) system yielded ages around 51.5 Ma that have been interpreted as the age of subduction initiation (Ishizuka et al., 2011; Reagan et al., 2013). This indicates that melts forming the oceanic crust in a fore-arc spreading environment during subduction initiation are compositionally more akin to depleted mid-ocean ridge basalts and become more boninitic as subduction progressed with melting of more depleted mantle (Reagan et al., 2013).

A V/Yb diagram is used to show the effect of oxygen fugacity from MORB to Island Arc Tholeiites (IAT). V is more incompatible in the higher oxidation states and this causes more V to be partitioned into the magma (Pearce, 2014; Pearce & Parkinson, 1993). V/Yb contents of the isolated dykes from the study area are presented in Figure 13. MORB magmas are thought to be generated in relatively reducing conditions (quartz-fayalite-magnetite buffer: QFM-1) whereas oceanic arc magmas are generated at higher oxygen fugacity (quartz-fayalite-magnetite buffer: QFM + 1) (Ballhaus, 1993; Kelley & Cottrell, 2012; Pearce & Parkinson, 1993). The Group I dykes display oxygen fugacities around the QFM trend, transitional between MORB and IAT, whereas the low-Ti

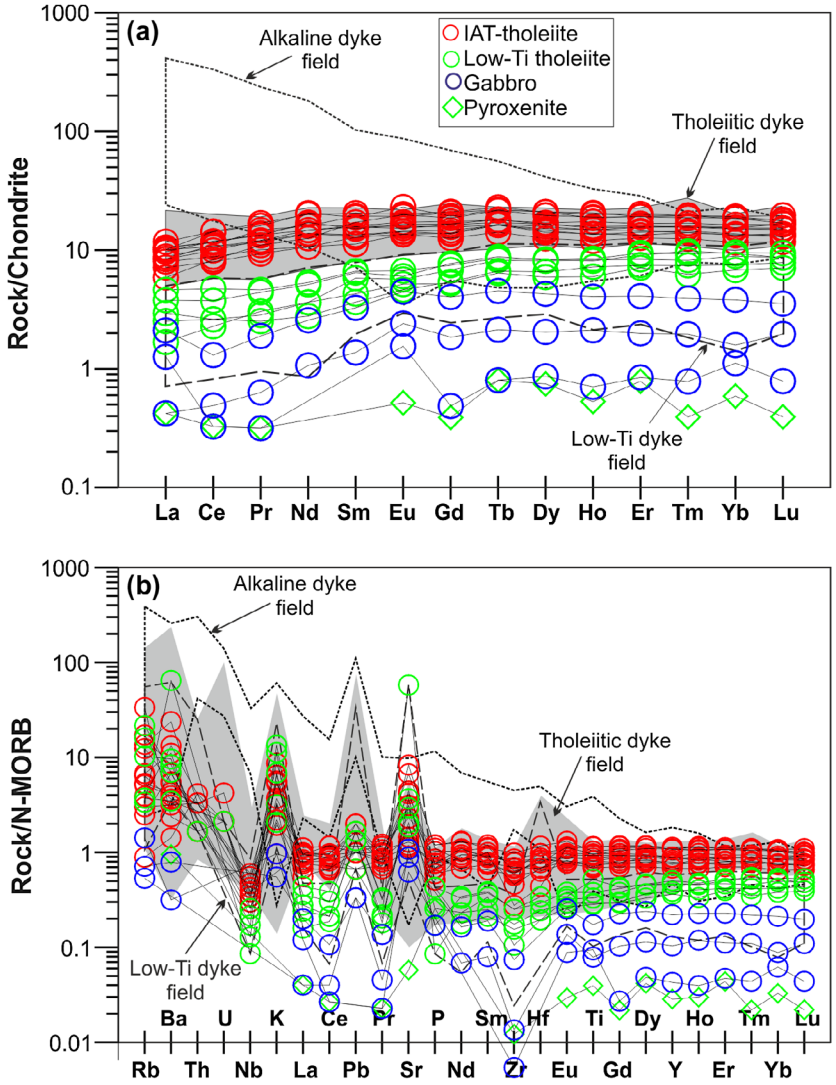


Figure 10. (a) Chondrite normalized REE and N-MORB normalized multi-element diagrams for the isolated diabase dykes, cumulate gabbro and pyroxenite dyke (Normalizing values are from Sun & McDonough, 1989). Data for the isolated dykes of the Tauride ophiolites are the same as in Figure 7.

Group II dykes plot above and along the QFM + 1 trend, suggesting higher oxygen fugacity in an island arc setting (Figure 13).

Major and trace element concentrations of the cumulate gabbros and pyroxenite dyke are presented in Table 3. The cumulate gabbros have low TiO_2 (.1–.22 wt.%), K_2O (.04–.07 wt.%), P_2O_5 (.02 wt.%), large-ion lithophile (LIL) elements such as Ba (2–9 ppm), Rb (.3–.8 ppm), other incompatible elements, i.e. Zr (.4–5.5 ppm), Y (.2–6.2 ppm), and REE. In contrast, the concentrations of Al_2O_3 (14.67–26.61 wt.%), CaO (12.59–15.95 wt.%) and MgO (9.38–15.84 wt.%) are high (Table 3). The gabbro (TO-7) sample has exceptionally high Al_2O_3 and low FeO*, suggesting that it contains a very high proportion of plagioclase. Whereas the olivine gabbro samples (TO-8 and 10) have high MgO, Cr and low Al_2O_3, suggesting high proportion of olivine. The gabbronorite (TO-18) sample has high Al_2O_3, MgO, FeO* and CaO, suggesting high proportion of plagioclase, clinopyroxene and orthopyroxene phases. The low concentrations of the incompatible trace elements (i.e. Cs, Hf, Nb, Ta, Th, U and rare earths) in Table 3 are attributed to the high proportion of cumulus minerals and low amounts of intercumulus-trapped liquid in the magma chamber. The major (Al_2O_3, MgO, CaO) and trace (Ni, Cr, Co, Sr) element geochemistry of gabbroic cumulates suggest that olivine, spinel, clinopyroxene and plagioclase fractionation played an important role within a magma chamber during their genesis at the base of an intra-oceanic arc setting. Similar features were reported from the cumulate rocks of the Mersin, Pozantı-Karsantı, Kızıldağ (Hatay) and Tekirova (Antalya) ophiolites (Bağcı, Parlak, & Höck, 2005; Bağcı et al., 2006; Parlak et al., 1996, 2000, 2002). The pyroxenite dyke cutting the mantle tectonite is characterized by low contents of TiO_2 (.05 wt%), LIL and high-field strength (HFS) elements, whereas it is rich in Ni (134.5 ppm), Cr (.42 wt.%), MgO (20.37 wt.%) and CaO (20.04 wt.%) (Table 1). Low Nb/Y ratios in the cumulate rocks (.02–.04) are characteristic of subalkaline (tholeiitic) basalts (Winchester & Floyd, 1977). Major element compositions of the cumulate gabbros, pyroxenite

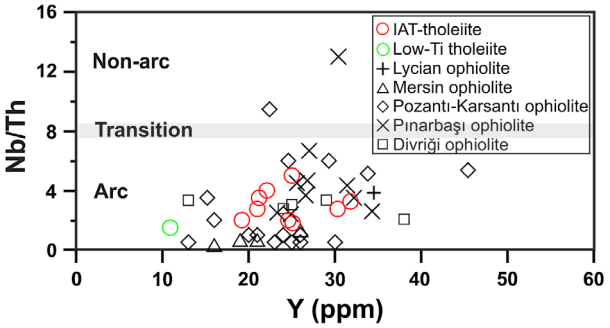


Figure 11. Nb/Th vs. Y diagram (after Jenner et al., 1991) for the isolated diabase dykes. Data for the isolated dykes of the Tauride ophiolites are the same as in Figure 7.

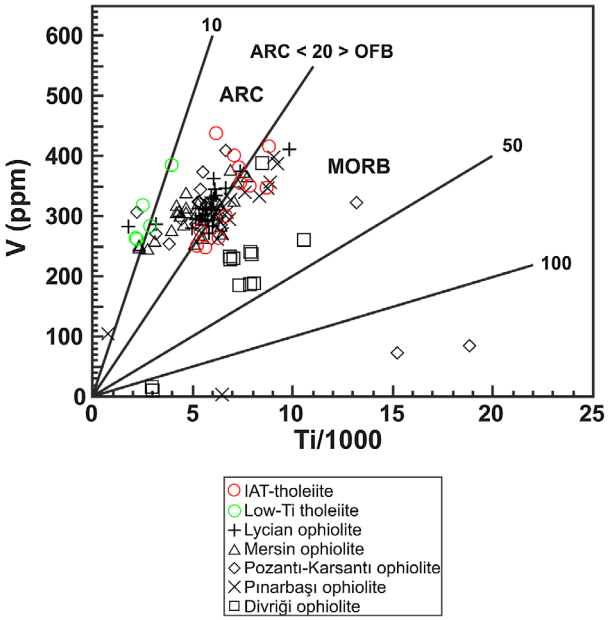


Figure 12. V vs. Ti variations for the isolated dykes from the study area (after Shervais, 1982). Data for the isolated dykes of the Tauride ophiolites are the same as in Figure 7.

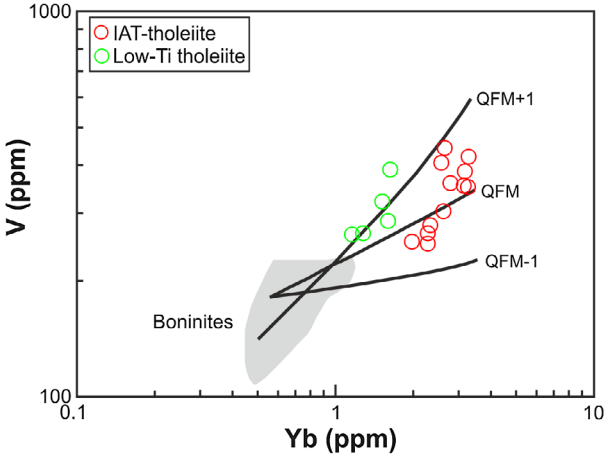


Figure 13. Plot of V vs. Yb for the isolated dykes (after Pearce & Parkinson, 1993, QFM = Quartz-Fayalite-Magnetite buffer).

dyke and isolated dykes are plotted on the AFM diagram of Beard (1986) (Figure 14). The cumulate rocks and pyroxenite dyke plot in the arc-related cumulate field

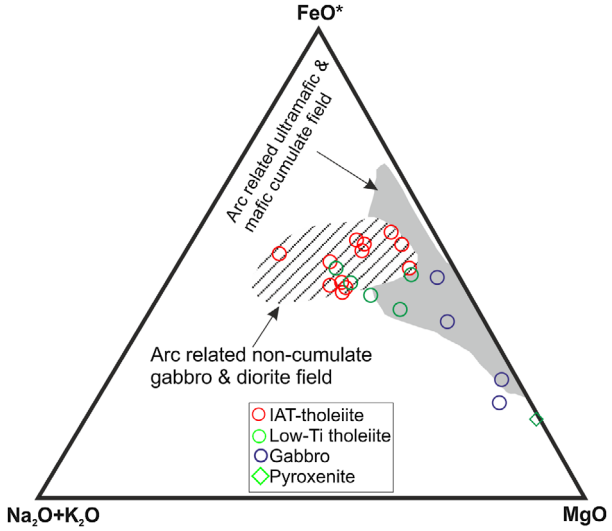


Figure 14. AFM composition of the cumulate and non-cumulate mafic-ultramafic rocks from the study area. Fields of cumulate and non-cumulate rocks are from Beard (1986).

whereas the isolated diabase dykes plot in the arc-related non-cumulate field (Figure 14). This implies that both the cumulate and non-cumulate mafic-ultramafic rocks formed in a subduction-related tectonic setting. Rare earth element (REE) concentrations of three cumulate gabbros and one pyroxenite sample are given in Table 3. Overall, they display more depleted REE patterns than the isolated dykes (Figure 10(a) and (b)). The cumulate rocks exhibit slightly depleted light rare earth element (LREE) to flat heavy rare earth (HREE) element patterns (La/Yb_N = .3–1.1) and overall REE abundances of between ×5 and ×.3 chondritic (Figure 10(a)). The pyroxenite dyke within the mantle tectonites exhibit the most-depleted REE patterns, with overall REE abundance from ×.3 to ×.8 chondritic and flat patterns (La/Yb_N = .72). The N-MORB normalized multi-element diagram for the gabbros and pyroxenite also confirms their depleted nature (Figure 10(b)).

5. Discussion & conclusion

The ophiolitic rocks from the southern margin of the Sivas basin, south of the Tecer Mountain area are thought to be the northwestern extension of the Divriği (Sivas) ophiolite, cropping out between Çetinkaya and Divriği towns (Sivas). The Divriği ophiolite formed in a suprasubduction zone setting during the late Cretaceous and was emplaced onto the Tauride platform (Parlak et al., 2006; Parlak, Karaoğlan, Rızaoğlu, Klötzli, et al., 2013).

Other ophiolites along the Tauride platform (the Lycian nappes, Tekirova, Beyşehir-Hoyran nappes, Mersin, Alihoca, Pozantı-Karsantı, Pınarbaşı and Divriği) originated in different oceanic basins, namely the İzmir-Ankara-Erzincan ocean, the Inner Tauride ocean and the Southern Neotethys. The Lycian nappes (Köyceğiz/Yeşilova ophiolites and associated mélanges) at the western end of

Taurides, are interpreted to have been derived from the northerly Neotethyan oceanic basin (Collins & Robertson, 1997, 1998, 1999). The Antalya Complex, including the Tekirova ophiolite, has been compared with the Troodos ophiolite (Cyprus), the Baer-Bassit ophiolite (northern Syria) and the Kızıldağ (Hatay) ophiolite. These ophiolites originated within the Southern Neotethys (Çetinkaplan et al., 2016; Robertson & Waldron, 1990; Robertson & Woodcock, 1981a, 1981b, 1981c, 1982; Robertson et al., 2012). The Beyşehir-Hoyran Nappes further to the east originated near the southern margin of the Inner Tauride Ocean and reached their present position by out-of-sequence thrusting in the Late Cretaceous (Andrew & Robertson, 2002). The Mersin, the Pozantı-Karsantı, the Alihoca ophiolites and associated units were rooted in the Inner Tauride Ocean that evolved between the Kırşehir massif/Central Anatolian Crystalline Complex to the north and the Tauride platform to the south and were thrust southwards onto the Tauride platform (Dilek & Whitney, 1997; Dilek et al., 1999; Lytwyn & Casey, 1995; Parlak & Robertson, 2004; Polat & Casey, 1995; Polat, Casey, & Kerrich, 1996). The Pınarbaşı (Kayseri) and the Divriği (Sivas) ophiolites formed by spreading above a northward-dipping, intra-oceanic subduction zone within the Inner Tauride Ocean and were emplaced onto the East Tauride platform as a result of trench-margin collision during the latest Cretaceous (Parlak et al., 2006; Robertson, Parlak, Metin, et al., 2013; Vergili & Parlak, 2005).

The Inner Tauride Ocean is believed to have separated the Tauride-Anatolide block from the Central Anatolian Crystalline Complex (Andrew & Robertson, 2002; Dilek et al., 1999; Görür, Tüysüz, & Şengör, 1998; Görür et al., 1984; Okay & Tüysüz, 1999; Pourteau et al., 2010; Robertson et al., 2009). This oceanic basin was consumed as a result of north-dipping subduction and closed during the latest Cretaceous to early Cenozoic times. There are number of arguments supporting the existence of the Inner Tauride suture, evolved during the Late Triassic to Eocene, between the Central Anatolian Crystalline Complex and the Tauride-Anatolide Block such as; (a) contrasting metamorphic histories of the Central Anatolian Crystalline Complex and the Tauride-Anatolide Block (Dilek & Whitney, 1997; Fayon, Whitney, Teyssier, Garver, & Dilek, 2001; Okay, Harris, & Kelley, 1998; Pourteau et al., 2010; Robertson et al., 2009; Seaton, Whitney, Teyssier, Toraman, & Heizler, 2009; Sherlock, Kelley, Inger, Harris, & Okay, 1999; Whitney & Dilek, 1998; Whitney & Hamilton, 2004; Whitney, Teyssier, Dilek, & Fayon, 2001; Whitney, Teyssier, Fayon, Hamilton, & Heizler, 2003), (b) late Cretaceous I-type calc-alkaline granitoids from the western margin of the Central Anatolian Crystalline Complex (Kadıoğlu, Dilek, & Foland, 2006), (c) well- preserved metamorphic soles with a consistent late Cretaceous (92–93 Ma) ages compared to the ophiolites of the İzmir-Ankara-Erzincan suture zone (Çelik et al., 2006, 2011; Parlak & Delaloye, 1999; Parlak, Çolakoğlu, et al., 2013; Parlak et al., 2006), (d) existence of blueschist blocks within unmetamorphosed melanges associated with some of the Tauride-Anatolide ophiolites (Droop, Karakaya, Eren, & Karakaya, 2005; Göncüoğlu, Özcan, Turhan, & Işık, 1992; van der Kaaden, 1966; Okay, 1982; Pourteau et al., 2010; Rimmelé, 2003), (e) the Tauride-Anatolide continent, a good example of a subducted, exhumed passive margin within a collisional orogen (Robertson et al., 2009), (f) the arc-related setting of the volcanics within the post-collisional basins (i.e. Ulukışla) covering the southern margin of the Central Anatolian Crystalline Complex (Andrew & Robertson, 2002; Clark & Robertson, 2002; Gökten, 1993; Gökten & Floyd, 1987; Görür et al., 1984, 1998).

Petrological studies of the mantle tectonites of the Tauride ophiolites show that two types of mantle residues, such as Mid-Ocean Ridge (MOR) and Suprasubduction zone (SSZ) type exist, suggesting a low degree of partial melting in a mid-ocean ridge environment during the opening stage of the Neotethyan oceanic basins, followed by re-melting and depletion in a suprasubduction zone (SSZ) setting (Aldanmaz, Schmidt, Gourgaud, & Meisel, 2009; Caran, Çoban, Flower, Ottley, & Yılmaz, 2010; Saka, Uysal, Akmaz, Kaliwoda, & Hochleitner, 2014; Uysal et al., 2012). The crustal rocks (i.e. isotropic to cumulate gabbro, sheeted dykes) of the ophiolites along the Taurides suggest that they were mainly derived from island arc tholeiitic melts in a SSZ setting (Bağcı et al., 2006; Parlak et al., 1996, 2000, 2002). Individual dyke emplacement in mantle tectonites, tectonically underlying metamorphic soles as well as crustal rocks of the ophiolites along the Tauride belt, is a conspicuous feature. These individual dykes were not observed within the ophiolitic melanges, suggesting that they intruded prior to mélange formation and after ophiolite emplacement onto the Tauride platform. Individual dykes were observed to be undeformed or unmetamorphosed after their emplacement. The petrology of isolated dykes along the Tauride belt suggests that they originated from depleted or enriched mantle sources as a result of either (a) ridge-subduction (Lytwyn & Casey, 1995; Polat et al., 1996), or (b) slab break-off (Çelik, 2007; Parlak et al., 2006), or (c) multiple intra-oceanic thrusting and emplacement in small oceanic basins (Çelik, 2007; Çelik & Chiaradia, 2008) and (d) asymmetrical ridge collapse (Dilek et al., 1999).

Parlak (2016) suggested that subduction initiation and roll-back processes (Stern & Bloomer, 1992) could best explain the structural and petrological relationships of the ophiolite genesis, metamorphic sole formation and subsequent dyke emplacement along the Tauride mountain range. During subduction initiation, mainly OIB-like alkaline and MORB-type tholeiitic basalts were accreted to the base of the overriding oceanic plate and metamorphosed under amphibolite facies conditions between about 96–90 Ma ago, based on ^{40}Ar–^{39}Ar ages. Following the subduction initiation and metamorphic sole formation, old and dense lithosphere sinking into the asthenosphere rolled back and the metamorphic

sole was attached to the base of the overriding plate. Hot asthenosphere flowed upward into the region above the sinking plate margin. Crustal formation was fed by melts, including both boninitic (high-Mg andesites) to island arc tholeiitic magmas, leaving a refractory harzburgitic mantle residue. After ~2 Ma, post-metamorphic isolated dykes intruded the metamorphic sole and the overlying oceanic lithosphere (91–86 Ma; ^{40}Ar–^{39}Ar data). Late stage dykes with enriched compositions are interpreted to have been derived from local fractures or tears in the subducting plate rather than large-scale breakoff.

The geochemistry of the isolated dykes cutting the mantle tectonites in the studied region clearly show that they were derived from a tholeiitic magma in a suprasubduction zone (SSZ) setting within the Inner Tauride Ocean in the Late Cretaceous. The REE and multi-element diagrams, as well as trace element (i.e. V, Ti) contents, suggest that the isolated dykes are characterized by two subgroups, namely the Group I normal tholeiitic dykes and the Group II low-Ti tholeiitic dykes, suggesting progressive source depletion in a SSZ setting. Melting of the mantle in the presence of water makes the melting process more oxidising and that in turn increases the proportion of vanadium in the higher oxidation states. Because V is more incompatible in the higher oxidation states, this causes more vanadium to be partitioned into the magma. Thus, subducted water leads to a melting regime that produces magmas with not just lower Ti but also higher V (Pearce, 2014; Pearce & Parkinson, 1993). The V–Ti diagram of Shervais (1982) clearly shows that the V/Ti ratio is low in MORB, intermediate island arc tholeiites (IAT) and high in boninites. Pearce (2014) stated that subduction-initiation ophiolites commonly form a distinct time trend on the V/Ti diagram of Shervais (1982): from more MORB-like when subduction begins, to more IAT-like as subduction influence increases, to more boninite-like as the slab subducts far enough to act as a barrier to mantle flow. The isolated dykes in the study area exhibit relatively higher oxygen fugacities (Figure 13) and suggest their origin was from an intra-oceanic subduction related setting. The major and trace element (including REE) geochemistry of the mafic cumulate rocks suggests that the primary magma was compositionally similar to those observed in modern island-arc tholeiitic sequences and the eastern Mediterranean ophiolites.

The isolated dykes cutting the metamorphic sole and the mantle tectonites in the Divriği (Sivas) region yielded a 75.9 ± .30 Ma ^{40}Ar–^{39}Ar cooling age (Parlak, Karaoğlan, Rızaoğlu, Klötzli, et al., 2013), and exhibit an alkaline (Nb/Y = .68–2.11) character, geochemically similar to within-plate alkaline basalts (Parlak et al., 2006). Whereas the crustal rocks (cumulates, isotrope gabbro and sheeted dykes) of the Divriği ophiolite are tholeiitic in composition and geochemically depleted in nature (Parlak, Yılmaz, Boztuğ, & Höck, 2005). They formed in a suprasubduction zone tectonic setting north of the Tauride platform in the Late Cretaceous (~90 Ma) (Parlak et al., 2005; Parlak, Karaoğlan, Rızaoğlu, Klötzli, et al., 2013). Its alkaline isolated dykes were probably the result of late-stage magmatism fed by melts that originated within an asthenospheric window due to slab break-off, shortly before the emplacement onto the Tauride platform to the south (Parlak et al., 2006). This may suggest that melts with enriched and depleted compositions were effective during the crustal architecture above an intraoceanic subduction zone for the Divriği ophiolite and the ophiolite in the Tecer Mountain area.

The ophiolitic rocks from the southern margin of the Sivas basin around the Tecer Mountains and the Divriği (Sivas) region exhibit number of similarities. (a) They display a common tectono-stratigraphy from bottom to top (Tauride platform, melange and ophiolite). (b) The ophiolites in the region namely the Pınarbaşı (Kayseri), Gürün, Divriği (Sivas), Kuluncak, Hekimhan (Malatya), Dağlıca (Afşin-Kahramanmaraş) were interpreted as fragments of regional-scale thrust sheet of emplaced SSZ-type oceanic lithosphere onto the Eastern Tauride carbonate platform during latest Cretaceous time and displaced by later tectonics and suture tightening (Robertson, Parlak, Metin, et al., 2013). (c) Robertson, Parlak, Metin, et al. (2013) stated that the Taurides as a whole exhibit a common palaeogeography and tectonic evolution during Triassic-Eocene time. (d) Mesozoic carbonate platform and continental margin units in the Divriği (Sivas) region are interpreted as rifted northern margin of the Tauride-Anatolide microcontinent bordering the Inner Tauride Ocean in the north (Robertson, Parlak, Metin, et al., 2013). All the evidence suggests that the ophiolites and related rocks in the southern margin of the Sivas basin around Tecer Mauntain area and Divriği (Sivas) region were derived from an oceanic basin, so called Inner Tauride Ocean, to the north of the Tauride platform.

The tholeiitic isolated dykes cutting the mantle tectonites in the Tecer Mountain area differ from the alkaline isolated dykes cutting the Divriği ophiolite. Since the late stage dykes (~76 Ma) in the Divriği (Sivas) area are alkaline in nature, the tholeiitic composition of the isolated dykes in the present study suggests that they were emplaced prior to the alkaline dykes during Late Cretaceous (~90 Ma) SSZ-spreading.

Acknowledgement

We are grateful to two anonymous reviewers and Erdin Bozkurt for their valuable comments that improved the quality of the manuscript.

Disclosure statement

No potential conflict of interest was reported by the authors.

Funding

This study was supported by the Scientific and Technological Research Council of Turkey [grant number TÜBİTAK-ÇAYDAG: 107Y146].

ORCID

Osman Parlak http://orcid.org/0000-0002-4652-3902

References

Alabaster, T., Pearce, J. A., & Malpas, J. (1982). The volcanic stratigraphy and petrogenesis of the Oman ophiolite complex. *Contributions to Mineralogy and Petrology, 81*, 168–183.

Aldanmaz, E., Schmidt, M. W., Gourgaud, A., & Meisel, T. (2009). Mid-ocean ridge and supra-subduction geochemical signatures in spinel-peridotites from the Neotethyan ophiolites in SW Turkey: Implications for upper mantle melting processes. *Lithos, 113*, 691–708.

Al-Riyami, K., Robertson, A. H. F., Dixon, J., & Xenophontos, C. (2002). Origin and emplacement of the Late Cretaceous Baer-Bassit ophiolite and its metamorphic sole in NW Syria. *Lithos, 65*, 225–260.

Andrew, T., & Robertson, A. H. F. (2002). The Beyşehir-Hoyran-Hadim Nappes: Genesis and emplacement of Mesozoic marginal and oceanic units of the northern Neotethys in southern Turkey. *Journal of the Geological Society, 159*, 529–543.

Arculus, R. J., & Powell, R. (1986). Source component mixing in the regions of arc magma generation. *Journal of Geophysical Research, 91*, 5913–5926.

Atabey, E., & Aktimur, H. T. (1997). *1:100.000 geological map of Turkey*. 48, (Sivas-G24). Ankara: MTA.

Bağcı, U., & Parlak, O. (2009). Petrology of the Tekirova (Antalya) ophiolite (Southern Turkey): Evidence for diverse magma generations and their tectonic implications during Neotethyan-subduction. *International Journal of Earth Sciences, 98*, 387–405.

Bağcı, U., Parlak, O., & Höck, V. (2005). Whole rock and mineral chemistry of cumulates from the Kızıldağ (Hatay) ophiolite (Turkey): Clues for multiple magma generation during crustal accretion in the southern Neotethyan ocean. *Mineralogical Magazine, 69*, 53–76.

Bağcı, U., Parlak, O., & Höck, V. (2006). Geochemical character and tectonic environment of ultramafic to mafic cumulates from the Tekirova (Antalya) ophiolite (southern Turkey). *Geological Journal, 41*, 193–219.

Bağcı, U., Parlak, O., & Höck, V. (2008). Geochemistry and tectonic environment of diverse magma generations forming the crustal units of the Kızıldağ (Hatay) ophiolites southern Turkey. *Turkish Journal of Earth Sciences, 17*, 43–71.

Ballhaus, C. (1993). Redox states of lithospheric and asthenospheric upper mantle. *Contributions to Mineralogy and Petrology, 114*, 331–348.

Beard, J. S. (1986). Characteristic mineralogy of arc-related cumulate gabbros: Implications for the tectonic setting of gabbroic plutons and for andesite genesis. *Geology, 14*, 848–851.

Beccaluva, L., Coltorti, M., Giunta, G., & Siena, F. (2004). Tethyan vs. Cordilleran ophiolites: A reappraisal of distinctive tectono-magmatic features of supra-subduction complexes in relation to the subduction mode. *Tectonophysics, 393*, 163–174.

Beccaluva, L., Coltorti, M., Saccani, E., & Siena, F. (2005). Magma generation and crustal accretion as evidenced by supra-subduction ophiolites of the Albanide-Hellenide Subpelagonian zone. *The Island Arc, 14*, 551–563.

Caran, Ş., Çoban, H., Flower, M. F. J., Ottley, C. J., & Yılmaz, K. (2010). Podiform chromitites and mantle peridotites of the Antalya ophiolite, Isparta Angle (SW Turkey): Implications for partial melting and melt-rock interaction in oceanic and subduction-related settings. *Lithos, 114*, 307–326.

Çelik, Ö. F. (2007). Metamorphic sole rocks and their mafic dykes in the eastern Tauride belt ophiolites (southern Turkey): İmplications for OIB type magma generation following slab break-off. *Geological Magazine, 144*, 849–866.

Çelik, Ö. F. (2008). Detailed geochemistry and K-Ar geochronology of the metamorphic sole rocks and their mafic dykes from the Mersin ophiolite, southern Turkey. *Turkish Journal of Earth Sciences, 17*, 685–708.

Çelik, Ö. F., & Chiaradia, M. (2008). Geochemical and petrological aspects of dyke intrusions in the Lycian ophiolites (SW Turkey): A case study for the dyke emplacement along the Tauride Belt Ophiolites. *International Journal of Earth Sciences, 97*, 1151–1164.

Çelik, Ö. F., & Delaloye, M. (2003). Origin of metamorphic soles and their post-kinematic mafic dyke swarms in the Antalya and Lycian ophiolites, SW Turkey. *Geological Journal, 38*, 235–256.

Çelik, Ö. F., Delaloye, M., & Feraud, G. (2006). Precise ^{40}Ar-^{39}Ar ages from the metamorphic sole rocks of the Tauride Belt Ophiolites, southern Turkey: İmplications for the rapid cooling history. *Geological Magazine, 143*, 213–227.

Çelik, Ö. F., Marzoli, A., Marschik, R., Chiaradia, M., Neubauer, N., & Öz, İ. (2011). Early-middle Jurassic intraoceanic subduction in the İzmir-Ankara-Erzincan Ocean, northern Turkey. *Tectonophysics, 509*, 120–134.

Çetinkaplan, M., Pourteau, A., Candan, O., Koralay, O. E., Oberhänsli, R., Okay, A. I., … Şengün, F. (2016). P-T-t evolution of eclogite/blueschist facies metamorphism in Alanya Massif: Time and space relations with HP event in Bitlis Massif, Turkey. *International Journal of Earth Sciences, 105*, 247–281.

Clark, M., & Robertson, A. H. F. (2002). The role of the Early Tertiary Ulukisla Basin, southern Turkey, in suturing of the Mesozoic Tethys ocean. *Journal of the Geological Society, 159*, 673–690.

Collins, A. S., & Robertson, A. H. F. (1997). Lycian melange, southwestern Turkey: An emplaced Late Cretaceous accretionary complex. *Geology, 25*, 255–258.

Collins, A. S., & Robertson, A. H. F. (1998). Processes of Late Cretaceous to Late Miocene episodic thrust sheet translation in the Lycian Taurides, SW Turkey. *Journal of the Geological Society, 155*, 759–772.

Collins, A. S., & Robertson, A. H. F. (1999). Evolution of the Lycian Allochthon, western Turkey, as a North-facing Late Palaeozoic to Mesozoic rift and passive continental margin. *Geological Journal, 34*, 107–138.

Dilek, Y., & Flower, M. F. J. (2003). Arc-trench rollback and forearc accretion: 2. A model template for Ophiolites in Albania, Cyprus, and Oman. In Y. Dilek, & P. T. Robinson (Eds.), *Ophiolites in Earth history* (Vol. 218, pp. 43–68). London: Geological Society, Special Publications.

Dilek, Y., & Thy, P. (2006). Age and petrogenesis of plagiogranite intrusions in the Ankara melange, central Turkey. *Island Arc, 15*, 44–57.

Dilek, Y., & Thy, P. (2009). Island arc tholeiite to boninitic melt evolution of the Cretaceous Kizildag (Turkey) ophiolite: Model for multi-stage early arc–forearc magmatism in Tethyan subduction factories. *Lithos, 113*, 68–87.

Dilek, Y., & Whitney, D. L. (1997). Counterclockwise P-T-t trajectory from the metamorphic sole of a Neo-Tethyan ophiolite (Turkey). *Tectonophysics, 280*, 295–310.

Dilek, Y., Thy, P., Hacker, B. R., & Grundvig, S. (1999). Structure and petrology of Tauride ophiolites and mafic dike intrusions (Turkey): Implications for the Neotethyan ocean. *Geological Society of America Bulletin, 111*, 1192–1216.

Dilek, Y., Furnes, H., & Shallo, M. (2008). Geochemistry of the Jurassic Mirdita Ophiolite (Albania) and the MORB to SSZ evolution of a marginal basin oceanic crust. *Lithos, 100*, 174–209.

Droop, G. T. R., Karakaya, M. C., Eren, Y., & Karakaya, N. (2005). Metamorphic evolution of blueschists of the Altınekin Complex, Konya area, south central Turkey. *Geological Journal, 40*, 127–153.

Elitok, Ö. (2001). Geochemistry and tectonic significance of the Şarkikaraağaç ophiolites in the Beyşehir-Hoyran Nappes, SW Turkey. In Ö. Akıncı, M. Görmüş, M. Kuşçu, R. Karagüzel, & M. Bozcu (Eds.), *Proceedings of the 4th International Symposium on Eastern Mediterranean Geology*, 21–25 May 2001 Isparta, Turkey, pp. 181–196.

Elitok, Ö., & Drüppel, K. (2008). Geochemistry and tectonic significance of metamorphic sole rocks beneath the Beyşehir-Hoyran ophiolite (SW-Turkey). *Lithos, 100*, 322–353.

Fayon, A. K., Whitney, D. L., Teyssier, C., Garver, J. I., & Dilek, Y. (2001). Effects of plate convergence obliquity on timing and mechanisms of exhumation of a mid-crustal terrain, the Central Anatolian Crystalline Complex. *Earth and Planetary Science Letters, 192*, 191–205.

Floyd, P. A., & Winchester, J. A. (1978). Identification and discrimination of altered and metamorphosed volcanic rocks using immobile elements. *Chemical Geology, 21*, 291–306.

Gökten, E. (1993). Geology of the southern boundary of the Sivas Basin in the east of Ulaş (Sivas–central Anatolia): Tectonic development related to the closure of inner Tauride Ocean. *Turkish Association of Petroleum Geologist Bulletin, 5*, 35–55.

Gökten, E., & Floyd, P. A. (1987). Geochemistry and tectonic environment of the Şarkışla area volcanic rocks in Central Anatolia, Turkey. *Mineralogical Magazine, 51*, 553–559.

Göncüoğlu, M. C., Özcan, A., Turhan, N., & Işık, A. (1992). *Stratigraphy of the Kütahya region*. ISGB-92. Field Guide Book 3. Ankara, Turkey: MTA.

Göncüoğlu, M. C., Dirik, K., & Kozlu, H. (1996–1997). Pre-alpine and alpine terranes in Turkey: Explanatory notes to the terrane map of Turkey. *Annalles Geologiques des Pays Hellenique, 37*, 1–3.

Görür, N., Oktay, F. Y., Seymen, İ., & Şengör, A. M. C. (1984). Palaeotectonic evolution of the Tuzgölü basin complex, Central Turkey: Sedimentary record of a Neotethyan closure. In J. A. Dixon, & A. H. F. Robertson (Eds.), *The Geological Evolution of the Eastern Mediterranean* (Vol. 17, pp. 467–482). London: Geological Society, Special Publications.

Görür, N., Tüysüz, O., & Şengör, A. M. C. (1998). Tectonic evolution of the central Anatolian basins. *International Geology Review, 40*, 831–850.

Gust, D. A., & Johnson, R. W. (1981). Amphibole bearing cumulates from Boisa island, Papua New Guinea: Evaluation of the role of fractional crystallization in an andesitic volcano. *Journal of Geology, 89*, 219–232.

Hall, C. E., Gurnis, M., Sdrolias, M., Lavier, L. L., & Müller, R. D. (2003). Catastrophic initiation of subduction following forced convergence across fracture zones. *Earth and Planetary Science Letters, 212*, 15–30.

Hart, S. R., Erlank, A. J., & Kable, E. J. D. (1974). Sea floor basalt alteration: Some chemical and Sr isotopic effects. *Contributions to Mineralogy and Petrology, 44*, 219–230.

van Hinsbergen, D. J. J., Maffione, M., Plunder, A., Kaymakcı, N., Ganerød, M., Hendriks, B. W. H., … Vissers, R. L. M. (2016). Tectonic evolution and paleogeography of the Kırşehir Block and the Central Anatolian Ophiolites, Turkey. *Tectonics, 35*, 983–1014.

Humphris, S. E., & Thompson, G. (1978). Trace element mobility during hydrothermal alteration of oceanic basalts. *Geochimica et Cosmochimica Acta, 42*, 127–136.

İnan, S., & İnan, N. (1987). Tecer kireçtaşı formasyonunun stratigrafik tanımlanması. *Cumhuriyet Üniversitesi Mühendislik Fakültesi Dergisi, Yerbilimleri, 4*, 13–22.

Ishizuka, O., Tani, K., Reagan, M. K., Kanayama, K., Umino, S., Harigane, Y., … Dunkley, D. J. (2011). The timescales of subduction initiation and subsequent evolution of an oceanic island arc. *Earth and Planetary Science Letters, 306*, 229–240.

Jakes, P., & Gill, J. (1970). Rare earth elements and the island arc tholeiitic series. *Earth Planetary Science Letters, 9*, 17–28.

Jenner, G. A., Dunning, G. R., Malpas, J., Brown, M., & Brace, T. (1991). Bay of Islands and Little Port complexes, revisited: Age, geochemical and isotopic evidence confirm suprasubduction-zone origin. *Canadian Journal of Earth Sciences, 28*, 1635–1652.

van der Kaaden, G. (1966). Importance and distribution of glaucophane bearing rocks in Turkey. *Maden Tetkik ve Arama Enstitüsü Dergisi, 67*, 38–69.

Kadıoğlu, Y. K., Dilek, Y., & Foland, K. A. (2006). Slab breakoff and syncollisional origin of the Late Cretaceous magmatism in the Central Anatolian Crystalline Complex, Turkey. In Y. Dilek, & S. Pavlides (Eds.), *Postcollisional tectonics and magmatism in the Mediterranean Region and Asia* (Vol. 409, pp. 381–415). Boulder, CO: Geological Society of America Special Paper.

Karaoğlan, F., Parlak, O., Klötzli, U., Thöni, M., & Koller, F. (2012). U-Pb and Sm–Nd geochronology of the ophiolites from the SE Turkey: İmplications for the Neotethyan evolution. *Geodinamica Acta, 25*, 146–161.

Karaoğlan, F., Parlak, O., Klötzlı, U., Thönı, M., & Koller, F. (2013). U-Pb and Sm-Nd geochronology of the Kızıldağ (Hatay, Turkey) ophiolite: İmplications for the timing and duration of suprasubduction zone type oceanic crust formation in the southern Neotethys. *Geological Magazine, 150*, 283–299.

Karaoğlan, F., Parlak, O., Klötzli, U., Koller, F., & Rızaoğlu, T. (2013). Age and duration of intra-oceanic arc volcanism built on a suprasubduction zone type oceanic crust in southern Neotethys, SE Anatolia. *Geoscience Frontiers, 4*, 399–408.

Kavak, K. Ş. (2010). *Sivas havzası güney kenarının ASTER uydu görüntüleriyle incelenmesi ve spektral kütüphanesinin oluşturulması*. Tübitak projesi, 107Y146, 128 pp

Kelley, K. A., & Cottrell, E. (2012). The influence of magmatic differentiation on the oxidation state of Fe in a basaltic arc magma. *Earth and Planetary Science Letters, 329–330*, 109–121.

Koglin, N. (2008). *Geochemistry, petrogenesis and tectonic setting of Ophiolites and mafic-ultramafic complexes in the Northeastern Aegean Region: New trace-element, isotopic and age constraints* (Unpublished doctoral dissertation). Mainz, Germany.

Koglin, N., Kostopoulos, D., & Reischmann, T. (2009). Geochemistry, petrogenesis and tectonic setting of the Samothraki mafic suite, NE Greece: Trace-element, isotopic and zircon age constraints. *Tectonophysics, 473*, 53–68.

Konstantinou, A., Wirth, K. R., & Vervoort, J. (2007). U-Pb isotopic dating of Troodos plagiogranite, Cyprus by LA-ICP-MS. *GSA Annual Meeting, Geological Society of America, Abstracts with Programs, 39*, 388.

Liati, A., Gebauer, D., & Fanning, C. M. (2004). The age of ophiolitic rocks of the Hellenides (Vourinos, Pindos, Crete): First U-Pb ion microprobe (SHRIMP) zircon ages. *Chemical Geology, 207*, 171–188.

Lytwyn, J. N., & Casey, J. F. (1995). The geochemistry of postkinematic mafic dike swarms and subophiolitic metabasites, Pozanti-Karsanti ophiolite, Turkey: Evidence for ridge subduction. *Geological Society of America Bulletin, 107*, 830–850.

Meffre, S., Aitchison, J., & Crawford, A. J. (1996). Geochemical evolution and tectonic significance of boninites and tholeiites from the Koh ophiolite, New Caledonia. *Tectonics, 15*, 67–83.

MTA. (2002). *1:500.000 ölçekli Türkiye jeoloji haritası* [Geological map of Turkey, 1:500.000]. Ankara: MadenTektik ve Arama Genel Müdürlüğü [General Directorate of Mineral Research and Exploration].

Mukasa, S. B., & Ludden, J. N. (1987). Uranium-lead isotopic ages of plagiogranites from the Troodos ophiolite, Cyprus, and their tectonic significance. *Geology, 15*, 825–828.

Okay, Aİ. (1982). Incipient blueschist metamorphism and metasomatism in the Tavşanlı Region, northwest Turkey. *Contributions to Mineralogy and Petrology, 79*, 361–367.

Okay, Aİ., & Tüysüz, O. (1999). Tethyan sutures of northern Turkey. In A. Mascle, & L. Jolivet (Eds.), *The Mediterranean basins: Tertiary extension within the Alpine Orogeny* (Vol. 156, pp. 475–516). London: Geological Society, Special Publications.

Okay, Aİ., Harris, N. B. W., & Kelley, S. (1998). Exhumation of blueschists along a Tethyan suture in northwest Turkey. *Tectonophysics, 285*, 275–299.

Parlak, O. (1996). *Geochemistry and geochronology of the Mersin ophiolite within the Eastern Mediterranean tectonic frame (Southern Turkey)* (Unpublished doctoral dissertation). University of Geneva, Switzerland.

Parlak, O. (2000). Geochemistry and significance of mafic dyke swarms in the Pozantı-Karsantı ophiolite (southern Turkey). *Turkish Journal of Earth Sciences, 24*, 29–38.

Parlak, O. (2016). The Tauride ophiolites of Anatolia (Turkey): A review. *Journal of Earth Science, 27*, 901–934.

Parlak, O., & Delaloye, M. (1996). Geochemistry and timing of post-metamorphic dyke emplacement in the Mersin ophiolite (southern Turkey): New age constraints from $^{40}Ar/^{39}Ar$ geochronology. *Terra Nova, 8*, 585–592.

Parlak, O., & Delaloye, M. (1999). Precise $^{40}Ar/^{39}Ar$ ages from the metamorphic sole of the Mersin ophiolite (southern Turkey). *Tectonophysics, 301*, 145–158.

Parlak, O., & Robertson, A. H. F. (2004). The ophiolite-related Mersin Melange, southern Turkey: Its role in the tectonicsedimentary setting of Tethys in the Eastern Mediterranean region. *Geological Magazine, 141*, 257–286.

Parlak, O., Delaloye, M., & Bingöl, E. (1995). Origin of subophiolitic metamorphic rocks beneath the Mersin ophiolite, southern Turkey. *Ofioliti, 20*, 97–110.

Parlak, O., Delaloye, M., & Bíngöl, E. (1996). Mineral chemistry of ultramafic and mafic cumulates as an indicator of the arc-related origin of the Mersin ophiolite (southern Turkey). *Geologische Rundschau, 85*, 647–661.

Parlak, O., Höck, V., Kozlu, H., & Delaloye, M. (2004). Oceanic crust generation in an island arc tectonic setting, SE Anatolian orogenic belt (Turkey). *Geological Magazine, 141*, 583–603.

Parlak, O., Höck, V., & Delaloye, M. (2000). Suprasubduction zone origin of the Pozanti-Karsanti ophiolite (southern Turkey) deduced from whole-rock and mineral chemistry of the gabbroic cumulates. In E. Bozkurt, J. A. Winchester, & J. D. A. Piper (Eds.), *Tectonics and magmatism in Turkey and the surrounding area* (Vol. 173, pp. 219–234). London: Geological Society, Special Publications.

Parlak, O., Höck, V., & Delaloye, M. (2002). The suprasubduction Pozanti-Karsanti ophiolite, southern Turkey: Evidence for high pressure crystal fractionation of ultramafic cumulates. *Lithos, 65*, 205–224.

Parlak, O., Yılmaz, H., Boztuğ, D., & Höck, V. (2005). *Geochemistry and tectonic setting of the Divriği ophiolite in the east central Anatolia (Sivas, Turkey): Evidence for melt generation within an asthenospheric window prior to ophiolite emplacement onto the Taurides*. International Symposium on the Geodynamics of Eastern Mediterranean: Active Tectonics of the Aegean Region, 15–18, June 2005. Turkey, İstanbul: Kadir Has University, p. 224.

Parlak, O., Yılmaz, H., & Boztuğ, D. (2006). Geochemistry and tectonic setting of the metamorphic sole rocks and isolated dykes from the Divriği ophiolite (Sivas, Turkey): Evidence for melt generation within an asthenospheric window prior to ophiolite emplacement. *Turkish Journal of Earth Sciences, 15*, 25–45.

Parlak, O., Rızaoğlu, T., Bağcı, U., Karaoğlan, F., & Höck, V. (2009). Tectonic significance of the geochemistry and petrology of ophiolites in southeast Anatolia, Turkey. *Tectonophysics, 473*, 173–187.

Parlak, O., Karaoğlan, F., Rızaoğlu, T., Klötzli, U., Koller, F., & Billor, Z. (2013). U-Pb and $^{40}Ar/^{39}Ar$ geochronology of the ophiolites and granitoids from the Tauride belt: İmplications for the evolution of the Inner Tauride suture. *Journal of Geodynamics, 65*, 22–37.

Parlak, O., Karaoğlan, F., Rızaoğlu, T., Nurlu, N., Bağcı, U., Höck, V., … Topak, Y. (2013). Petrology of the İspendere (Malatya) ophiolite from the Southeast Anatolia: Implications for the Late Mesozoic evolution of the southern Neotethyan ocean. In A. H. F. Robertson, O. Parlak, & U. C. Ünlügenç (Eds.), *Geological development of Anatolia and the Easternmost Mediterranean region* (Vol. 372, pp. 219–247). London: Geological Society, Special Publications.

Parlak, O., Çolakoğlu, A., Dönmez, C., Sayak, H., Türkel, A., Yıldırım, N., & Odabaşı, İ. (2013). Geochemistry and tectonic significance of Ophiolites along the İzmir-Ankara-Erzincan suture zone in Northeastern Anatolia. In A. H. F. Robertson, O. Parlak, & U. C. Ünlügenç (Eds.), *Geological development of Anatolia and the Easternmost Mediterranean region* (Vol. 372, pp. 75–105). London: Geological Society, Special Publications.

Pearce, J. A. (1982). Trace element characteristics of lavas from destructive plate boundaries. In R. S. Thorpe (Ed.), *Andesites* (pp. 525–548). New York, NY: Wiley.

Pearce, J. A. (1983). Role of the subcontinental lithosphere in magma genesis at active continental margins. In C. J. Hawkesworth, & M. J. Norry (Eds.), *Continental basalts and mantle xenoliths* (pp. 230–249). Cheshire: Shiva Publishing.

Pearce, J. A. (1996). A users guide to basalt discrimination diagrams. In D. A. Wyman (Ed.), *Trace element geochemistry of volcanic rocks: Applications for massive sulphide exploration* (Vol. 12, pp. 79–113). St. John's: Geochemistry, Geological Association of Canada, Short Course Notes.

Pearce, J. A. (2003). Supra-subduction zone ophiolites: The search for modern analogues. In Y. Dilek, & S. Newcomb (Eds.), *Ophiolite concept and the evolution of geological thought* (Vol. 373, pp. 269–293). Boulder, CO: Geological Society of America Special Paper.

Pearce, J. A. (2014). Immobile element fingerprinting of ophiolites. *Elements, 10*, 101–108.

Pearce, J. A., & Cann, J. R. (1973). Tectonic setting of basic volcanic rocks determined using trace element analyses. *Earth and Planetary Science Letters, 19*, 290–300.

Pearce, J. A., & Norry, M. J. (1979). Petrogenetic implications of Ti, Zr, Y and Nb variations in volcanic rocks. *Contributions to Mineralogy and Petrology, 69*, 33–47.

Pearce, J. A., & Parkinson, I. J. (1993). Trace element models of mantle melting: Application to volcanic arc petrogenesis. In H. M. Pichard, T. Alabaster, N. B. W. Harris, & C. R. Neary (Eds.), *Magmatic processes and plate tectonics* (Vol. 76, pp. 373–403). London: Geological Society, Special Publications.

Pe-Piper, G., Tsıkouras, B., & Hatzıpanagıotou, K. (2004). Evolution of boninites and island-arc tholeiites in the Pindos Ophiolite, Greece. *Geological Magazine, 141*, 455–469.

Polat, A., & Casey, J. F. (1995). A structural record of the emplacement of the Pozanti-Karsanti ophiolite onto the

Menderes-Taurus block in the late Cretaceous, eastern Taurides, Turkey. *Journal of Structural Geology, 17*, 1673–1688.
Polat, A., Casey, J. F., & Kerrich, R. (1996). Geochemical characteristics of accreted material beneath the Pozanti-Karsanti ophiolite, Turkey: Intra-oceanic detachment, assembly and obduction. *Tectonophysics, 263*, 249–276.
Pourteau, A., Candan, O., & Oberhänsli, R. (2010). High-pressure metasediments in central Turkey: Constraints on the Neotethyan closure history. *Tectonics, 29*, TC5004. doi:10.1029/2009TC002650
Reagan, M. K., Ishizuka, O., Stern, R. J., Kelley, K. A., Ohara, Y., Blichert-Toft, J., … Woods, M. (2010). Fore-arc basalts and subduction initiation in the Izu-Bonin-Mariana system. *Geochemistry Geophysics Geosystems, 11*, 1–17.
Reagan, M. K., McClelland, W. C., Girard, G., Goff, K. R., Peate, D. W., Ohara, Y., & Stern, R. J. (2013). The geology of the southern Mariana fore-arc crust: Implications for the scale of Eocene volcanism in the western Pacific. *Earth and Planetary Science Letters, 380*, 41–51.
Rimmelé, G. (2003). *Structural and metamorphic evolution of the Lycian Nappes and the Menderes Massif (southwest Turkey): Geodynamic implications and correlations with the Aegean Domain* (Unpublished doctoral dissertation). Potsdam, Germany.
Rızaoğlu, T., Parlak, O., Höck, V., & İşler, F. (2006). Nature and significance of Late Cretaceous ophiolitic rocks and its relation to the Baskil granitoid in Elazığ region, SE Turkey. In A. H. F. Robertson, & D. Mountrakis (Eds.), *Tectonic development of the Eastern Mediterranean region* (Vol. 260, pp. 327–350). London: Geological Society, Special Publications.
Robertson, A. H. F. (2002). Overview of the genesis and emplacement of Mesozoic ophiolites in the Eastern Mediterranean Tethyan region. *Lithos, 65*, 1–67.
Robertson, A. H. F., & Waldron, J. (1990). Geochemistry and tectonic setting of Late Triassic and Late Jurassic-early Cretaceous basaltic extrusives from the Antalya Complex, SW Turkey. In M. Y. Savaşçın, & A. H. Eronat (Eds.), *Proceedings of International Earth Science Congress on Aegean Regions* (Vol. 2, pp. 279–299). İzmir, Turkey: Dokuz Eylül University.
Robertson, A. H. F., & Woodcock, N. H. (1981a). Bilelyeri Group, Antalya Complex: Deposition on a Mesozoic passive continental margin, south-west Turkey. *Sedimentology, 28*, 381–399.
Robertson, A. H. F., & Woodcock, N. H. (1981b). Alakırçay Group, Antalya Complex, SW Turkey: A deformed Mesozoic carbonate margin. *Sedimentary Geology, 30*, 95–131.
Robertson, A. H. F., & Woodcock, N. H. (1981c). Gödene Zone, Antalya Complex SW Turkey: Volcanism and sedimentation on Mesozoic marginal ocean crust. *Geologische Rundschau, 70*, 1177–1214.
Robertson, A. H. F., & Woodcock, N. H. (1982). Sedimentary history of the southwestern segment of the Mesozoic-tertiary Antalya continental margin, southwestern Turkey. *Eclogae Geologica Helvetica, 75*, 517–562.
Robertson, A. H. F., Parlak, O., & Ustaömer, T. (2009). Melange genesis and ophiolite emplacement related to subduction of the northern margin of the Tauride-Anatolide continent, central and western Turkey. In D. J. J. Vanhinsbergen, M. A. Edwards, & R. Govers (Eds.), *Collision and collapse at the Africa-Arabia-Eurasia subduction zone* (Vol. 311, pp. 9–66). London: Geological Society, Special Publications.
Robertson, A. H. F., Parlak, O., & Ustaomer, T. (2012). Overview of the Palaeozoic-Neogene evolution of Neotethys in the Eastern Mediterranean region (southern Turkey, Cyprus, Syria). *Petroleum Geoscience, 18*, 381–404.
Robertson, A. H. F., Parlak, O., Metin, Y., Vergili, Ö., Taslı, K., İnan, N., & Soycan, H. (2013). Late Palaeozoic-Cenozoic tectonic development of carbonate platform, margin and oceanic units in the Eastern Taurides, Turkey. In A. H. F. Robertson, O. Parlak, & U. C. Ünlügenç (Eds.), *Geological development of Anatolia and the Easternmost Mediterranean region* (Vol. 372, pp. 167–218). London: Geological Society Special Publication.
Robertson, A. H. F., Parlak, O., Ustaömer, T., Taslı, K., İnan, N., Dumitrica, P., & Karaoğlan, F. (2013). Subduction, ophiolite genesis and collision history of Tethys adjacent to the Eurasian continental margin: New evidence from the Eastern Pontides, Turkey. *Geodinamica Acta, 26*, 230–293.
Rollinson, H. R. (1993). *Using geochemical data: Evaluation, presentation, Interpretation*. New York, NY: Wiley.
Saccani, E., & Photiades, A. (2005). Petrogenesis and tectonomagmatic significance of volcanic and subvolcanic rocks in the Albanide-Hellenide ophiolitic melanges. *The Island Arc, 14*, 494–516.
Saka, S., Uysal, I., Akmaz, R. M., Kaliwoda, M., & Hochleitner, R. (2014). The effects of partial melting, melt-mantle interaction and fractionation on ophiolite generation: Constraints from the late Cretaceous Pozantı-Karsantı ophiolite, southern Turkey. *Lithos, 202–203*, 300–316.
Sarıfakıoğlu, E., Dilek, Y., & Uysal, İ. (2012). *The Petrogenesis and Geodynamic Significance of Bahçe (Osmaniye) Ophiolite*. 5th Geochemistry Symposium (pp. 112–113). Denizli,Turkey.
Seaton, N. C. A., Whitney, D. L., Teyssier, C., Toraman, E., & Heizler, M. T. (2009). Recrystallization of high-pressure marble (Sivrihisar, Turkey). *Tectonophysics, 479*, 241–253.
Sherlock, S., Kelley, S. P., Inger, S., Harris, N., & Okay, Aİ. (1999). ^{40}Ar-^{39}Ar and Rb-Sr geochronology of high-pressure metamorphism and exhumation history of the Tavşanlı Zone, NW Turkey. *Contributions to Mineralgy and Petrology, 137*, 46–58.
Shervais, J. W. (1982). Ti-V plots and the petrogenesis of modern ophiolitic lavas. *Earth and Planetary Science Letters, 59*, 101–118.
Stern, R. J. (1979). On the origin of andesite in the northern Mariana Island arc: Implications from Agrigan. *Contributions to Mineralogy and Petrology, 68*, 207–219.
Stern, R. J., & Bloomer, S. H. (1992). Subduction zone infancy: Examples from the Eocene Izu-Bonin-Mariana and Jurassic California arcs. *Geological Society of America Bulletin, 104*, 1621–1636.
Sun, S. S., & McDonough, W. F. (1989). Chemical and isotopic systematics of oceanic basalts: Implications for mantle composition and proccesses. In A. D. Saunders, & M. J. Norry (Eds.), *Magmatism in oceanic basins* (Vol. 42, pp. 313–345). London: Geological Society, Special Publications.
Thompson, G. (1991). Metamorphic and hydrothermal processes: Basalt-seawater interactions. In P. A. Floyd (Ed.), *Oceanic basalts* (pp. 148–173). Glasgow and London: Blackie.
Topuz, G., Göçmengil, G., Rolland, Y., Çelik, Ö. F., Zack, T., & Schmitt, A. K. (2012). Jurassic accretionary and ophiolite from northeast Turkey: No evidence for the Cimmerian continental ribbon. *Geology, 41*, 255–258.
Uysal, İ., Ersoy, Y. E., Karslı, O., Dilek, Y., Sadıklar, M. B., Ottley, C. J., … Meisel, T. (2012). Coexistence of abyssal and ultra-depleted SSZ type mantle peridotites in a Neotethyan ophiolite in SW Turkey: Constraints from mineral composition, whole rock geochemistry (major-trace-REE-PGE), and Re-Os isotope systematics. *Lithos, 132–133*, 50–69.
Vergili, Ö., & Parlak, O. (2005). Geochemistry and tectonic setting of metamorphic sole rocks and mafic dykes from the Pınarbaşı (Kayseri) ophiolite, Central Anatolia. *Ofioliti, 30*, 37–52.
Wallin, E. T., & Metcalf, R. V. (1998). Supra-subduction zone ophiolite formed in an extensional forearc: Trinity Terrane,

Klamath mountains, California. *Journal of Geology, 106*, 591–608.

Whitney, D. L., & Dilek, Y. (1998). Metamorphism during Alpine crustal thickening and extension in Central Anatolia, Turkey: The Nigde metamorphic core complex. *Journal of Petrology, 39*, 1385–1403.

Whitney, D. L., & Hamilton, M. A. (2004). Timing of high-grade metamorphism in central Turkey and the assembly of Anatolia. *Journal of the Geological Society, 161*, 823–828.

Whitney, D. L., Teyssier, C., Dilek, Y., & Fayon, A. K. (2001). Metamorphism of the central Anatolian Crystalline Complex, Turkey: İnfluence of orogen-normal collision vs. wrench-dominated tectonics on P-T-t paths. *Journal of Metamorphic Geology, 19*, 411–432.

Whitney, D. L., Teyssier, C., Fayon, A. K., Hamilton, M. A., & Heizler, M. (2003). Tectonic controls on metamorphism, partial melting, and intrusion: Timing and duration of regional metamorphism and magmatism in the Niğde Massif, Turkey. *Tectonophysics, 376*, 37–60.

Winchester, J. A., & Floyd, P. A. (1977). Geochemical discrimination of different magma series and their differentiation products using immobile elements. *Chemical Geology, 20*, 325–343.

Wood, D. A., Joron, J. L., & Treuil, M. (1979). A re-appraisal of the use of trace elements to classify and discriminate between magma series erupted in different tectonic settings. *Earth and Planetary Science Letters, 45*, 326–336.

Yalınız, K. M., Floyd, P. A., & Göncüoğlu, M. C. (1996). Supra-subduction zone ophiolites of Central Anatolia: Geochemical evidence from the Sarikaraman ophiolite, Aksaray, Turkey. *Mineralogical Magazine, 60*, 697–710.

Yalınız, K. M., Floyd, P. A., & Göncüoğlu, M. C. (2000). Geochemistry of volcanic rocks from the Çiçekdağ Ophiolite, Central Anatolia, Turkey, and their inferred tectonic setting within the northern branch of the Neotethyan Ocean. In E. Bozkurt, J. A. Winchester, & J. D. A. Piper (Eds.), *Tectonics and mangamism in Turkey and the surrounding area* (Vol. 173, pp. 203–218). London: Geological Society, Special Publications.

Yılmaz, H., Arıkal, T., & Yılmaz, A. (2001). *Geology of the Güneş ophiolite (Divriği-Sivas)*. Proceedings of the 54th Geological Congress of Turkey, Ankara, pp. 54–65 (in Turkish with English Abstract).

Yogodzinski, G. M., Volynets, O. N., Koloskov, A. V., Seliverstov, N. I., & Matvenkov, V. V. (1993). Magnesian andesites and the subduction component in strongly calc-alkaline series at Piip volcano, far western Aleutians. *Journal of Petrology, 35*, 163–204.